Original Article

Lower MMP12 expression is likely to contribute to better effect of postoperative adjuvant transarterial chemoembolization via reducing MEK/ERK signaling activity in patients with hepatocellular carcinoma

Ai-Xin Ou^{1,2*}, Ying-Jie Di^{3*}, Lei Miao¹, Yin-Gen Luo¹, Ming-Rong Wang², Jia-Jie Hao², Xiao Li^{1,3}

¹Department of Interventional Therapy, National Cancer Center/National Clinical Research Center for Cancer/Cancer Hospital, Chinese Academy of Medical Sciences and Peking Union Medical College, Beijing 100021, P. R. China; ²State Key Laboratory of Molecular Oncology, Center for Cancer Precision Medicine, National Cancer Center/National Clinical Research Center for Cancer/Cancer Hospital, Chinese Academy of Medical Sciences and Peking Union Medical College, Beijing 100021, P. R. China; ³Department of Interventional Therapy, Shanxi Province Cancer Hospital, Shanxi Hospital Affiliated to Cancer Hospital, Chinese Academy of Medical Sciences, Cancer Hospital Affiliated to Shanxi Medical University, Taiyuan 030000, Shanxi, P. R. China. *Equal contributors.

Received June 28, 2025; Accepted October 15, 2025; Epub October 15, 2025; Published October 30, 2025

Abstract: Hepatocellular carcinoma (HCC) frequently recurs after hepatectomy. Transarterial chemoembolization (TACE) is a common adjuvant therapy; however, reliable indicators of its efficacy remain limited. This study aimed to evaluate the clinical significance of matrix metallopeptidase 12 (MMP12) in HCC patients undergoing postoperative adjuvant TACE (PA-TACE) and to explore potential strategies to enhance the efficacy of PA-TACE. A retrospective analysis was conducted on 225 HCC patients who received TACE and were categorized into prophylactic and recurrence TACE groups. Clinical data including liver function, tumor characteristics, and imaging findings were collected. Tissue samples were subjected to MMP12 immunohistochemical staining, and patients were further stratified according to MMP12 expression levels. Univariate and multivariate Cox regression analyses were performed to identify risk factors, and a nomogram was constructed for prognostic evaluation. The role of MMP12 in TACE for HCC was examined using Western blotting, RT-qPCR, mass spectrometry, Transwell, wound-healing, and colony formation assays. Kaplan-Meier curves demonstrated significantly better survival in the low-MMP12-expression group. Microvascular infiltration, alpha-fetoprotein (AFP) levels, and MMP12 expression were identified as independent risk predictors for survival. The nomogram derived from these factors exhibited high predictive accuracy (area under the curve: 0.750-0.959) across multiple time points. In vitro experiments revealed that targeting MMP12 inhibited HCC cell invasion, migration, and colony formation by blocking the MEK/ERK signaling pathway. The MMP12 inhibitor GM6001 enhanced the therapeutic effects of TACE. In conclusion, MMP12 was identified as a key and independent prognostic biomarker for PA-TACE in HCC patients. The prognostic model integrating MMP12, AFP, and microvascular infiltration may help identify patients most likely to benefit from PA-TACE. Targeting MMP12 to block the MEK/ERK pathway and suppress HCC cell malignancy highlights its potential as a therapeutic target to improve PA-TACE efficacy.

Keywords: Hepatocellular carcinoma, MMP12, transarterial chemoembolization, prognosis, risk factors

Introduction

Liver cancer is a highly aggressive malignancy with significant incidence and mortality rates [1, 2]. Hepatocellular carcinoma (HCC), which accounts for approximately 80% of primary liver cancer cases, is the most prevalent subtype [3]. Although radical hepatectomy remains the standard treatment for patients with HCC

and adequate liver function [4, 5], postoperative outcomes are often poor because of high recurrence rates [6]. Consequently, several adjuvant therapies have been developed to reduce relapse and improve overall survival (OS) [7, 8]. Given the multiple risk factors for recurrence, transarterial chemoembolization (TACE) is frequently used as an adjuvant treatment after radical resection of HCC [9]. By

directly delivering chemotherapeutic agents and embolic materials into the tumor-feeding artery, TACE effectively suppresses local tumor growth and reduces the risk of recurrence [10, 11]. However, the benefits of this strategy are not universal [12]. Clinical observations suggest that high-risk patients, such as those with elevated alpha-fetoprotein (AFP) levels, multiple tumors, or large tumors, may benefit from postoperative adjuvant TACE (PA-TACE) [13-15]. In contrast, some patients exhibit poor sensitivity to PA-TACE. Therefore, accurately identifying patients most likely to benefit from PA-TACE is essential for optimal postoperative management of HCC. Nevertheless, few studies have identified reliable biomarkers or developed robust and efficient predictive models for PA-TACE in patients with HCC, resulting in limited predictive accuracy. This underscores an urgent need for novel biomarkers and predictive models to support clinical decision-making, enable timely intervention, and ultimately improve patient outcomes.

Matrix metallopeptidase 12 (MMP12) is a key enzyme involved in various biological processes, including tissue remodelling, reproduction, and embryonic development [16, 17]. The role of MMP12 in liver cancer has recently become a major focus of research, particularly regarding tumor progression, immune evasion, and prognostic evaluation. Evidence indicates that MMP12 upregulates PD-L1 expression, thereby promoting liver cancer [18]. Moreover, MMP12 may enhance the infiltration of FOXP3+ regulatory T cells (Treg) into tumor tissues, facilitating tumor progression and immune escape in HCC [19]. MMP12 mRNA has been proposed as a potential prognostic biomarker for OS and tumor recurrence in patients undergoing hepatectomy [20]. Our recent findings suggest that elevated MMP12 levels in biopsy samples are associated with poor HCC prognosis following TACE [21]. Although the prognostic value of MMP12 expression in HCC has been established, its role and underlying mechanisms in regulating the efficacy of PA-TACE remain unclear. This study aimed to evaluate the clinical significance of MMP12 protein expression in PA-TACE for patients with HCC and to explore potential strategies to improve the efficacy of PA-TACE in HCC treatment.

Materials and methods

Patients and tissue samples

From April 2014 to June 2023, we retrospectively reviewed the clinical records of 255 patients with HCC who underwent TACE after surgery at the Cancer Hospital, Chinese Academy of Medical Sciences. Patient inclusion was based on a confirmed HCC diagnosis according to the Chinese Liver Cancer (CNLC) criteria [22]. All enrolled patients had undergone hepatectomy before TACE, did not receive systemic therapy during the TACE period, and did not undergo subsequent surgical procedures, including liver transplantation or repeat hepatectomy, after TACE. Exclusion criteria were as follows: (1) presence of liver metastases or non-HCC malignant tumors; (2) incomplete computed tomography data; and (3) loss to follow-up after TACE. Surgical resection specimens were collected to obtain surgical margin and tumor tissues. All patients provided written informed consent, and none received any treatment before surgery. This study was approved by the Ethics Committees of Peking Union Medical College, Chinese Academy of Medical Sciences, and the Cancer Hospital (Approval No. 2025012115102402).

Hepatectomy and adjuvant TACE

The appropriate hepatectomy method was determined according to the location and extent of the tumors. Specifically, anatomical hepatectomy involves removal of the entire liver segment containing the tumor, delineated by the portal vein branches supplying the affected segment. In contrast, non-anatomical hepatectomy involves excision of the tumor together with a margin of adjacent non-neoplastic liver tissue [23, 24]. Prophylactic TACE is typically performed approximately 1 month after surgery. For adjuvant TACE, the Seldinger technique was used to cannulate the femoral artery, followed by angiography to evaluate portal vein blood flow and detect tumor-related abnormalities. A microcatheter was then carefully advanced into the tumor-feeding arterial branch for embolization. lodized oil and microspheres constituted the primary embolic agents. The chemotherapy regimen included 10-80 mg of pirarubicin. Embolic agents were added as needed until adequate embolization was achieved. Post-TACE, patients were monitored for bleeding, post-puncture hematoma, and post-embolization syndrome. Symptomatic management was provided when necessary.

Post-TACE follow-up

TACE was administered to all enrolled patients, who were subsequently followed every 3 months after surgery and for 4-6 weeks after each TACE session. Follow-up assessments included liver imaging and laboratory testing. Additional TACE treatments were administered to patients who developed signs of abnormal tumor growth or new lesions. The follow-up period continued until September 2024 or the end of the study. Progression-free survival (PFS) and OS after TACE were defined as the study endpoints. PFS was defined as the interval from the first TACE treatment to disease progression, and OS as the interval from the first TACE treatment to death or the last follow-up in September 2024. Local tumor response to TACE was evaluated according to the updated Response Evaluation Criteria in Solid Tumors (RECIST) [25].

Immunohistochemical staining and scoring

As previously described [26], immunohistochemical (IHC) staining was performed on HCC tissues from patients who underwent PA-TACE. Tissue sections were incubated with primary antibodies against MMP12 (anti-MMP12, 1:200; Santa Cruz Biotechnology) for 1 hour. The intensity and distribution of immunostaining were independently evaluated in a blinded manner by two pathologists using the histochemistry score (H-score). The H-score was calculated as follows:

$$\begin{aligned} \text{H--score} &= \sum (p_{_{i}} \times i) \\ &= (\% \text{ of weak - intensity cells} \times 1) \\ &+ (\% \text{ of moderate - intensity cells} \times 2) \\ &+ (\% \text{ of strong - intensity cells} \times 3) \end{aligned}$$

Where i represents the staining intensity grade, and p_i denotes the percentage of positive cells at each intensity level [27-29]. A score of 0 was assigned to negative samples with no staining; a score of 1 to weak-positive cases with light yellow staining; a score of 2 to moderate-positive cases with brown-yellow staining; and a score of 3 to strong-positive cases with tan staining. Based on the median H-score, MMP12 immunoreactivity was classified into high-

expression (H-score \geq 46.3) and low-expression (H-score < 46.3) groups.

Cell culture and transfection

The SNU182, Huh7, HepG2, and PLC/PRF5 HCC cell lines were obtained from the American Type Culture Collection, Huh7, HepG2, and PLC/ PRF5 cells were cultured in Dulbecco's modified Eagle's medium supplemented with 10% fetal bovine serum (FBS; AusGeneX), whereas SNU182 cells were cultured in RPMI-1640 medium supplemented with 10% FBS. Cells under normoxic conditions were maintained at 37°C in a humidified incubator with 5% CO₂ and 21% O₂. For hypoxic culture, cells were incubated using the Ruskinn INVIVO, 300 (England), which generates a hypoxic and humid atmosphere at 37°C with 5% CO₂ and 1% O₂. To simulate the conditions of TACE treatment, we established an in vitro TACE model using 0.2 μM doxorubicin (Dox) combined with 1% 0₂. This model has been widely used to mimic the hypoxic and chemotherapeutic microenvironment encountered by HCC cells following TACE [30-33]. Transfection was performed using JetPRIME Transfection Reagent (101000046, Polyplus, France) according to the manufacturer's instructions. Small interfering RNAs (siR-NAs) supplied by GenePharma (Shanghai, China). The sequence of siRNAs targeting MMP12 include: 5'-GGCCAUUCUAGUGAUCCA-ATT-3' (siMMP12-1) and 5'-GCCUCUCUGCUG-AUGACAUTT-3' (siMMP12-2), and the sequence of non-silencing control siRNA is 5'-UUCU-CCGAACGUGUCACGUTT-3'. The empty vector pCMV-MCS-3×Flag (VP048) and overexpression plasmid pCMV-MCS-MMP12-3×Flag (MH-10653) were purchased from Beijing MailGene Biotechnology Co., Ltd.

Invasion and migration assays

For migration assays, HCC cells (1×10^5) suspended in 200 µL of serum-free medium were added to the upper chamber of Transwell inserts, and 600 µL of medium containing 10% FBS was added to the lower chamber as a chemoattractant. After 24 hours of incubation at 37°C, cells remaining on the upper surface of the membrane were removed with cotton swabs. The membranes were then fixed with methanol and stained with 0.5% crystal violet. Cells on the lower surface of the membrane were counted in randomly selected fields under

a microscope. For invasion assays, cells were seeded in the upper chambers precoated with Matrigel. The inserts contained membranes with 8 μm pores to allow cell invasion. The subsequent processing steps were identical to those described for the migration assay. Images of the migrated and invated cells were captured and number of cells per field counted using an inverted microscope (Olympus BX53) at 200× magnification.

Wound healing assay

Cells were seeded in six-well plates and cultured until reaching full confluence. A vertical scratch was then made across the cell monolayer using a sterile pipette tip, followed by washing with PBS to remove detached cells. The wounded areas were observed and imaged using an inverted microscope (Olympus BX53) at 40× magnification at designated time points. Wound closure was quantified using ImageJ software (version 1.51j8; NIH, USA).

Colony formation assay

Cells (1×10^3) were seeded in six-well plates and cultured until visible colonies formed. Colonies were then fixed, stained, imaged, and counted for quantitative analysis.

Reverse transcription quantitative real-time polymerase chain reaction (RT-qPCR)

Total RNA was extracted using the RNA Pure Tissue & Cell Kit (Cwbiotech) according to the manufacturer's instructions. cDNA was synthesized using the HiFiScript cDNA Synthesis Kit (Cwbiotech). RT-qPCR was performed using the TB Green™ Premix Ex Taq Kit (TaKaRa). Gene expression levels were calculated using the 2-△△Ct method, with glyceraldehyde-3-phosphate dehydrogenase (GAPDH) serving as the internal reference.

Western blotting

Total protein was extracted using radioimmunoprecipitation assay buffer (Applygen) supplemented with protease and phosphatase inhibitors (Bimake). Protein concentrations were quantified using the Pierce Bicinchoninic Acid Protein Assay Kit (Thermo). Equal amounts of protein were separated by SDS-PAGE and

transferred to polyvinylidene fluoride membranes. The membranes were incubated with the appropriate primary and secondary antibodies, and protein bands were visualized using an electrochemiluminescence detection reagent.

Mass spectrometry analysis

MMP12 knockdown HCC cell lines were treated with 0.2 µM Dox under 1% 0, to mimic TACE conditions. Sample preparation and data-independent acquisition mass spectrometry (DIA-MS) analyses were performed by Novogene Co., Ltd., as previously described [34]. Following enzymatic protein hydrolysis, peptides were separated by liquid chromatography. Deep DIA mode was applied on the Astral mass spectrometry platform for detection. Raw DIA data were analyzed using Biognosys Spectronaut v.9 to achieve MS2-based label-free quantification. Enrichment analyses for Kyoto Encyclopedia of Genes and Genomes (KEGG) pathways and Gene Ontology (GO) categories were performed using the clusterProfiler R package. Proteins were classified into molecular functions, cellular components, and biological processes using GO analysis. KEGG analysis revealed enrichment in key metabolic pathways and signaling networks. P values less than 0.05 were considered statistically significant. Western blotting was subsequently conducted to validate alterations in protein expression associated with relevant signaling pathways.

Statistical analysis

All statistical analyses and data visualizations were performed using R software (version 3.3.3; R Foundation for Statistical Computing, Vienna, Austria) and GraphPad Prism 8 (GraphPad Software, San Diego, CA, USA). Continuous variables were compared using the Student's t-test, and categorical variables were compared using the χ^2 test or Fisher's exact test, as appropriate. PFS and OS were assessed using Kaplan-Meier curves, and differences were evaluated with the log-rank test. Cox proportional hazards regression was used to identify risk factors for PFS and OS following TACE. Variables with P < 0.05 in univariate analysis were included in multivariate analysis. Significant risk factors were then incorporated into a prognostic grading system, and a nomogram

Table 1. Baseline characteristics of the HCC patients

Characteristics	TACE for pr	rophylaxis	Dualua	TACE for	P value		
Characteristics	H-Score < 46.3	H-Score ≥ 46.3	P value	H-Score < 46.3	H-Score ≥ 46.3	P value	
n	50	53		62	60		
Gender, n (%)			0.910			0.273	
Male	41 (39.8%)	43 (41.7%)		55 (45.1%)	49 (40.2%)		
Female	9 (8.7%)	10 (9.7%)		7 (5.7%)	11 (9%)		
Age (years), mean ± sd	57.5 ± 9.2323	59.377 ± 8.3464	0.281	57.452 ± 9.5345	58.25 ± 8.7287	0.631	
Hepatitis status, n (%)			0.545			0.881	
HBV	39 (37.9%)	44 (42.7%)		51 (41.8%)	51 (41.8%)		
HCV	3 (2.9%)	1 (1%)		3 (2.5%)	3 (2.5%)		
Other	8 (7.8%)	8 (7.8%)		8 (6.6%)	6 (4.9%)		
Cirrhosis, n (%)			0.135			0.986	
Yes	30 (29.1%)	24 (23.3%)		34 (27.9%)	33 (27%)		
No	20 (19.4%)	29 (28.2%)		28 (23%)	27 (22.1%)		
Tumor necrosis, n (%)			0.828			0.363	
Yes	18 (17.5%)	18 (17.5%)		19 (15.6%)	14 (11.5%)		
No	32 (31.1%)	35 (34%)		43 (35.2%)	46 (37.7%)		
Microvascular infiltration, n (%)			0.460			0.094	
MO	16 (15.5%)	23 (22.3%)		31 (25.4%)	30 (24.6%)		
M1	23 (22.3%)	19 (18.4%)		20 (16.4%)	11 (9%)		
M2	11 (10.7%)	11 (10.7%)		11 (9%)	19 (15.6%)		
ALT (U/L), median (IQR)	29.25 (22.525, 42.75)	29.55 (20.9, 38.875)	0.976	27.5 (21.25, 41.7)	27.5 (21, 39.025)	0.768	
AST (U/L), median (IQR)	29 (25, 42.575)	28 (21.925, 32.5)	0.227	28 (22.175, 38.2)	27 (22.525, 36.65)	0.623	
AFP (ng/mL), n (%)	15.28 (5.3975, 105.68)	43 (6.71, 412.4)	0.241	9.82 (3.4925, 159.55)	12.69 (3.8325, 126.32)	0.824	
< 400	37 (35.9%)	36 (35%)		50 (41%)	48 (39.3%)		
≥ 400	13 (12.6%)	17 (16.5%)		12 (9.8%)	12 (9.8%)		
Number of tumors, n (%)			0.224			0.345	
Unifocal	40 (38.8%)	47 (45.6%)		49 (40.2%)	43 (35.2%)		
Multifocal	10 (9.7%)	6 (5.8%)		13 (10.7%)	17 (13.9%)		
Maximum tumor size (cm), n (%)			0.059			0.174	
< 3	6 (5.8%)	14 (13.6%)		17 (13.9%)	20 (16.4%)		
3-5	21 (20.4%)	25 (24.3%)		23 (18.9%)	13 (10.7%)		
> 5	23 (22.3%)	14 (13.6%)		22 (18%)	27 (22.1%)		

Child-pugh Class, n (%)		0	.501		0.461
Α	50 (48.5%)	51 (49.5%)	62 (50.8%)	58 (47.5%)	
В	0 (0%)	2 (1.9%)	O (O%)	2 (1.6%)	
BCLC stage, n (%)		0	.289		0.296
Α	43 (41.7%)	49 (47.6%)	59 (48.4%)	53 (43.4%)	
В	7 (6.8%)	4 (3.9%)	3 (2.5%)	7 (5.7%)	

Abbreviations: AFP, alpha-fetoprotein; ALT, alanine aminotransferase; AST, aspartate aminotransferase; BCLC, Barcelona Clinic Liver Cancer; HBV, Hepatitis B Virus; HCV, Hepatitis C Virus; IQR, interquartile range; SD, standard error of the mean; TACE, transarterial chemoembolization.

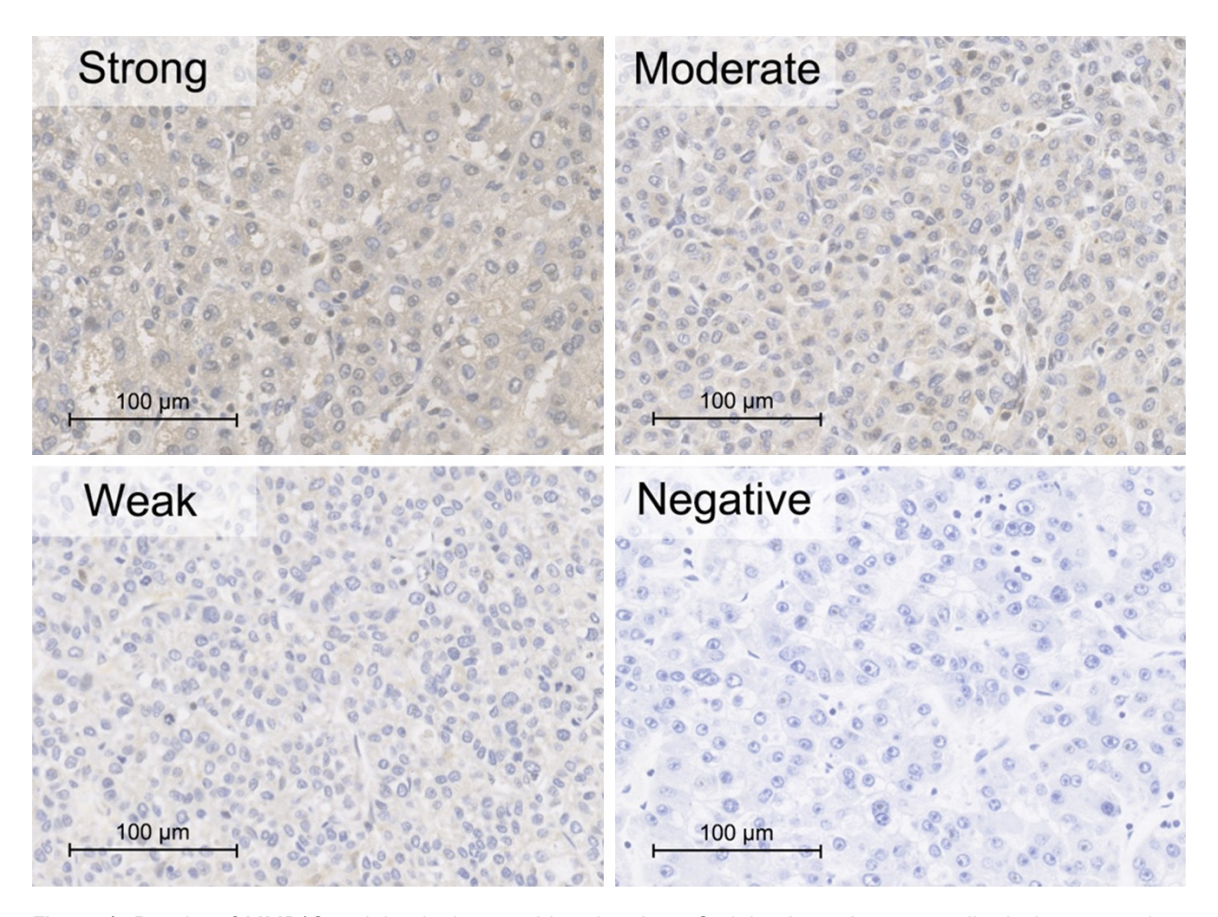


Figure 1. Results of MMP12 staining by immunohistochemistry. Staining intensity was qualitatively assessed as strong, moderate, weak or negative, original magnification 20×.

was constructed to predict PFS and OS in different risk groups. A two-tailed P value < 0.05 was considered statistically significant.

Results

The expression of MMP12 protein in patients with HCC treated with TACE after surgery

A total of 225 patients with HCC underwent TACE following surgery; 103 were included in the prophylactic TACE group, and 122 were included in the recurrence TACE group. **Table 1** summarizes the clinical characteristics of all patients included in this study. Most patients were male (83.5%), hepatitis B surface antigenpositive (82.2%), and had cirrhosis (53.7%).

MMP12 immunostaining was observed in the cytoplasm of tumor cells (**Figure 1**). Overall, the staining intensity of MMP12 in HCC varied widely, ranging from weak to strong (**Figure 1**). In addition, the proportion of tumor cells that were MMP12-positive ranged from 2.08% to 94.34%, and the H-score ranged from 3.33

to 225.22. Immunohistochemical analysis of tumor tissues from 225 patients revealed negative expression (H-score < 10) in 13 cases (5.8%), weak expression (H-score 10-46.3) in 99 cases (44.0%), moderate expression (H-score 46.3-150) in 107 cases (47.5%), and high expression (H-score 150-225.22) in six cases (2.7%).

To evaluate the role of MMP12 expression in HCC, the 225 patients were further stratified into two groups according to the median H-score of immunohistochemical staining intensity: H-score < 46.3 (n = 112) and H-score \geq 46.3 (n = 113). No significant differences were detected between these two groups in baseline clinical characteristics. By the end of the study period, 77 patients (34.2%) had died.

Comparison of PFS after TACE in H-score < 46.3 group and ≥ 46.3 group

Kaplan-Meier curves indicated that PFS was significantly higher in the H-score < 46.3 group than in the H-score ≥ 46.3 group, both in the

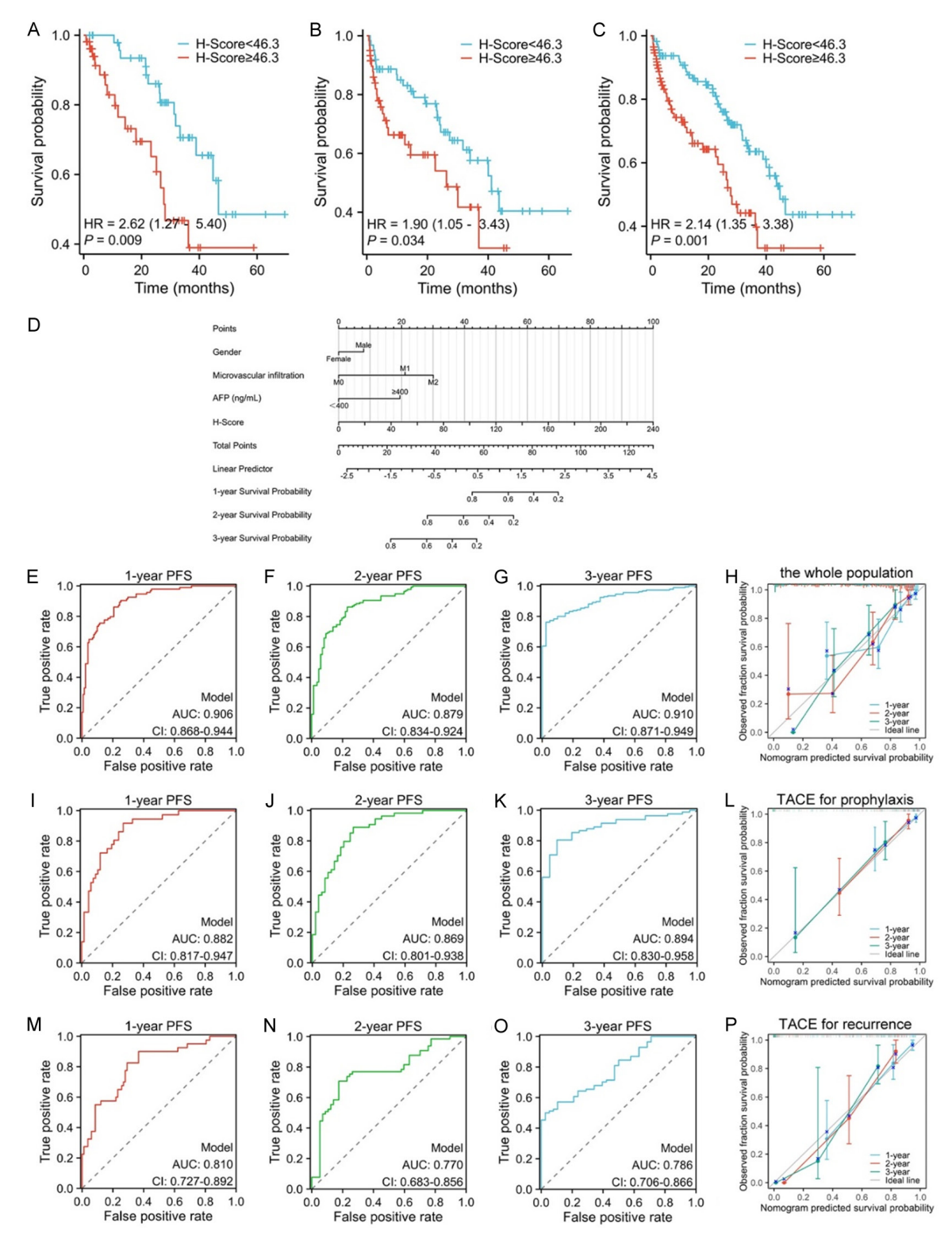


Figure 2. Predictive value of MMP12 for PFS in PA-TACE patients. Kaplan-Meier curves for PFS of the H-score < 46.3 and H-score \ge 46.3 groups in the TACE group for prophylaxis (A) and TACE group for recurrence (B) and in the whole population (C). (D) Nomogram of the predictive model for PFS of the whole population PFS. ROC curves to evaluate the accuracy of the prediction model based on the overall population (E-G), the TACE group for prophylaxis (I-K) and the TACE group for recurrence (M-O). Calibration plots to assess the calibration of the prediction model based on the overall population (H), the TACE group for prophylaxis (L) and the TACE group for recurrence (P).

TACE for prophylaxis group (HR = 2.62, 95% CI: 1.27-5.40; log-rank P = 0.009) (**Figure 2A**) and in the TACE for recurrence group (HR = 1.90, 95% CI: 1.05-3.43; log-rank P = 0.034) (**Figure 2B**). Similar results were observed in the overall population combining both groups (HR = 2.14, 95% CI: 1.35-3.38; log-rank P = 0.001) (**Figure 2C**).

The clinical data of the two subgroups were analyzed using Cox univariate regression, and variables with P < 0.05 were included in multivariate Cox regression after adjusting for confounding factors. The results showed that M1 (HR = 4.806, 95% CI: 1.884-12.257, P = 0.001),M2 (HR = 6.253, 95% CI: 2.047-19.107, P = 0.001), AFP (HR = 4.748, 95% CI: 2.000-11.273, $P \le 0.001$), and H-score (HR = 1.030, 95% CI: 1.018-1.042, P < 0.001) were independent risk factors for PFS in the TACE for prophylaxis group (Table 2). For the TACE recurrence group, tumor necrosis (HR = 0.494, 95% CI: 0.249-0.982, P = 0.044), M1 (HR = 2.743, 95% CI: 1.085-6.936, P = 0.033), M2 (HR = 4.108, 95% CI: 1.535-10.990, P = 0.005), ALT (HR = 1.002, 95% CI: (1.000-1.004), P = 0.023), AFP ng/mL (HR = 4.011, 95% CI: 1.705-9.440, P = 0.001), and H-score (HR = 1.020, 95% CI: 1.010-1.030, P < 0.001) were identified as independent risk factors for PFS (Table 2).

Similarly, Cox regression analyses were performed on the clinical data of all patients. The results indicated that M1 (HR = 2.987, 95% CI: 1.698-5.256, P < 0.001), M2 (HR = 4.824, 95% CI: 2.542-9.157, P < 0.001), AFP (HR = 3.291, 95% CI: 1.933-5.603, P < 0.001), and H-score (HR = 1.022, 95% CI: 1.015-1.028, P < 0.001) were independent risk factors for PFS in the overall cohort (**Table 4**).

Based on the multivariate analysis of all patients, a nomogram was constructed (Figure 2D), and its predictive performance was assessed using receiver operating characteristic (ROC) curves and calibration plots. The ROC curves demonstrated that the model achieved high predictive accuracy at all three time points (1, 2 and 3 year), with area under the curve (AUC) values of 0.906, 0.879, and 0.910, respectively (Figure 2E-G). Calibration plots also showed good agreement between the predicted and observed outcomes, indicating good predictive performance (Figure 2H). To verify the stability of the model, we analyzed the prog-

nostic model derived from the cohort in two subgroups: TACE for the prophylaxis group and TACE for the recurrence group. The results showed that the AUC values for the prophylaxis group were 0.882, 0.869, and 0.894 at 1, 2, and 3 years, respectively (Figure 2I-K). The AUC values of the recurrence group at the corresponding time points were 0.810, 0.770, and 0.786, respectively (Figure 2M-O). In additionally, the calibration curves showed satisfactory outcomes (Figure 2L, 2P).

Comparison of OS after TACE in H-score < 46.3 group and \geq 46.3 group

Kaplan-Meier curves revealed that the OS rate in the H-score < 46.3 group was significantly higher than that in the H-score \geq 46.3 group, both in the TACE for prophylaxis group (HR = 3.15, 95% CI: 1.48-6.72; log-rank P = 0.003) (**Figure 3A**) and in the TACE for recurrence group (HR = 2.31, 95% CI: 1.26-4.22; log-rank P = 0.007) (**Figure 3B**). Similar results were observed in the overall population comprising both groups (HR = 2.54, 95% CI: 1.59-4.08; log-rank P < 0.001) (**Figure 3C**).

Clinical data from the two subgroups were analyzed using Cox univariate regression, and variables with P < 0.05 were subsequently included in multivariate Cox regression after adjusting for confounding factors. The results showed that M1 (HR = 3.084, 95% CI: 1.271-7.482, P = 0.013), M2 (HR = 3.658, 95% CI: 1.207-11.086, P = 0.022), AFP (HR = 2.626, 95% CI: 1.113-6.199, P = 0.028), and H-score (HR = 1.023). 95% CI: 1.013-1.032, P < 0.001) were independent risk factors for OS in the TACE for prophylaxis group (Table 3). For the TACE recurrence group, M1 (HR = 3.523, 95% CI: 1.423-8.725, P = 0.006), M2 (HR = 3.322, 95% CI: 1.246-8.858, P = 0.016), AFP (HR = 9.733, 95% CI: 4.044-23.427, P < 0.001), and H-score (HR = 1.032, 95% CI: 1.020-1.043, P < 0.001) were identified as independent risk factors for OS (Table 3).

Similarly, Cox regression analyses were performed on the clinical data of all patients. The results indicated that M1 (HR = 2.480, 95% CI: 1.431-4.299, P = 0.001), M2 (HR = 3.703, 95% CI: 1.929-7.109, P < 0.001), AFP (HR = 2.972, 95% CI: 1.744-5.065, P < 0.001), and H-score (HR = 1.020, 95% CI: 1.015-1.026, P < 0.001)

Table 2. Univariable and multivariable analysis of factors associated correlated with PFS for prophylaxis and recurrence groups

		orophylaxis	TACE for recurrence					
Characteristics	Univariate analysis (PFS)		Multivariate analysis (PFS)		Univariate analysis (PFS)		Multivariate analysis (PFS)	
	Hazard ratio (95% CI)	P value	Hazard ratio (95% CI)	P value	Hazard ratio (95% CI)	P value	Hazard ratio (95% CI)	P value
Gender								
Male	Reference				Reference			
Female	1.142 (0.436-2.987)	0.787			1.024 (0.433-2.420)	0.957		
Age (years)	1.007 (0.963-1.052)	0.773			1.002 (0.971-1.033)	0.921		
Hepatitis status								
HBV	Reference				Reference			
HCV	2.830 (0.659-12.151)	0.162			0.449 (0.062-3.278)	0.430		
Other	0.816 (0.283-2.353)	0.706			1.002 (0.395-2.541)	0.996		
Cirrhosis								
Yes	Reference				Reference			
No	1.014 (0.498-2.064)	0.970			0.747 (0.413-1.353)	0.336		
Tumor necrosis								
Yes	Reference				Reference		Reference	
No	1.010 (0.483-2.113)	0.980			0.430 (0.239-0.773)	0.005	0.537 (0.273-1.054)	0.071
Microvascular infiltration								
MO	Reference		Reference		Reference		Reference	
M1	2.870 (1.200-6.867)	0.018	4.806 (1.884-12.257)	0.001	2.964 (1.313-6.691)	0.009	2.743 (1.085-6.936)	0.033
M2	5.540 (1.872-16.399)	0.002	6.253 (2.047-19.107)	0.001	9.276 (4.059-21.198)	< 0.001	4.108 (1.535-10.990)	0.005
ALT (U/L)	0.994 (0.981-1.006)	0.322			1.003 (1.000-1.005)	0.022	1.002 (1.000-1.004)	0.023
AST (U/L)	0.994 (0.980-1.007)	0.369			0.999 (0.993-1.005)	0.807		
AFP (ng/mL)								
<400	Reference				Reference		Reference	
≥ 400	6.134 (2.643-14.237)	< 0.001	4.748 (2.000-11.273)	< 0.001	6.226 (3.142-12.334)	< 0.001	4.011 (1.705-9.440)	0.001
Number of tumors								
Unifocal	Reference				Reference			
Multifocal	1.284 (0.526-3.135)	0.584			1.413 (0.753-2.652)	0.282		
Maximum tumor size (cm)								
< 3	Reference				Reference		Reference	
3-5	0.820 (0.330-2.034)	0.668			2.624 (1.192-5.778)	0.017	2.291 (0.974-5.388)	0.057
> 5	0.680 (0.258-1.790)	0.435			3.581 (1.580-8.118)	0.002	1.812 (0.698-4.702)	0.222
Child-pugh Class								
Α	Reference				Reference			
В	0.000 (0.000-Inf)	0.998			4.614 (0.612-34.822)	0.138		

BCLC stage

Α	Reference				Reference			
В	0.483 (0.114-2.039)	0.322			0.905 (0.323-2.535)	0.849		
H-Score	1.026 (1.016-1.037)	< 0.001	1.030 (1.018-1.042)	< 0.001	1.018 (1.009-1.026)	< 0.001	1.020 (1.010-1.030)	< 0.001

Abbreviations: AFP, alpha-fetoprotein; ALT, alanine aminotransferase; AST, aspartate aminotransferase; BCLC, Barcelona Clinic Liver Cancer; HBV, Hepatitis B Virus; HCV, Hepatitis C Virus; TACE, transarterial chemoembolization.

Table 3. Univariable and multivariable analysis of factors correlated associated with OS for prophylaxis and recurrence groups

		TACE for p	rophylaxis		TACE for recurrence			
Characteristics	Univariate analysis (OS)		Multivariate analysis (OS)		Univariate analysis (OS)		Multivariate analysis (OS)	
	Hazard ratio (95% CI)	P value	Hazard ratio (95% CI)	P value	Hazard ratio (95% CI)	P value	Hazard ratio (95% CI)	P value
Gender								
Male	Reference				Reference			
Female	1.110 (0.425-2.899)	0.831			1.104 (0.466-2.616)	0.821		
Age (years)	1.002 (0.961-1.045)	0.910			0.999 (0.969-1.030)	0.953		
Hepatitis status								
HBV	Reference				Reference			
HCV	1.839 (0.431-7.849)	0.411			0.593 (0.081-4.346)	0.607		
Other	0.730 (0.253-2.106)	0.560			1.156 (0.456-2.933)	0.760		
Cirrhosis								
Yes	Reference				Reference			
No	1.130 (0.553-2.309)	0.738			0.870 (0.481-1.575)	0.646		
Tumor necrosis								
Yes	Reference				Reference		Reference	
No	0.812 (0.388-1.700)	0.580			0.435 (0.242-0.780)	0.005	0.553 (0.272-1.127)	0.103
Microvascular infiltration								
MO	Reference		Reference		Reference		Reference	
M1	2.677 (1.140-6.288)	0.024	3.084 (1.271-7.482)	0.013	2.593 (1.220-5.513)	0.013	3.523 (1.423-8.725)	0.006
M2	4.748 (1.660-13.586)	0.004	3.658 (1.207-11.086)	0.022	6.452 (3.105-13.403)	< 0.001	3.322 (1.246-8.858)	0.016
ALT (U/L)	0.995 (0.983-1.008)	0.446			1.001 (1.000-1.002)	0.019	1.000 (0.999-1.002)	0.334
AST (U/L)	0.995 (0.980-1.010)	0.491			0.997 (0.990-1.005)	0.523		
AFP (ng/mL)								
<400	Reference		Reference		Reference		Reference	
≥ 400	4.915 (2.259 - 10.693)	< 0.001	2.626 (1.113-6.199)	0.028	6.805 (3.411-13.580)	< 0.001	9.733 (4.044-23.427)	< 0.001
Number of tumors								
Unifocal	Reference				Reference			
Multifocal	1.069 (0.437-2.613)	0.883			1.440 (0.767-2.702)	0.256		
Multilocal	1.069 (0.437-2.613)	0.003			1.440 (0.767-2.702)	0.256		

Maximum tumor size (cm)								
< 3	Reference				Reference		Reference	
3-5	0.687 (0.276-1.711)	0.420			2.320 (1.068-5.040)	0.033	2.256 (0.990-5.142)	0.053
> 5	0.671 (0.254-1.770)	0.420			2.343 (1.077-5.096)	0.032	1.219 (0.503-2.958)	0.661
Child-pugh Class								
A	Reference				Reference			
В	0.000 (0.000-Inf)	0.997			5.005 (0.669-37.451)	0.117		
BCLC stage								
A	Reference				Reference			
В	0.349 (0.082-1.478)	0.153			1.111 (0.398-3.102)	0.841		
H-Score	1.024 (1.015-1.033)	< 0.001	1.023 (1.013-1.032)	< 0.001	1.020 (1.011-1.028)	< 0.001	1.032 (1.020-1.043)	< 0.001

Abbreviations: AFP, alpha-fetoprotein; ALT, alanine aminotransferase; AST, aspartate aminotransferase; BCLC, Barcelona Clinic Liver Cancer; HBV, Hepatitis B Virus; HCV, Hepatitis C Virus; TACE, transarterial chemoembolization.

Table 4. Univariable and multivariable analysis of factors associated with PFS and OS for the whole population

	The whole population			The whole population				
Characteristics	Univariate analysis	(PFS)	Multivariate analys	is (PFS)	Univariate analysis	s (OS)	Multivariate analys	is (0S)
	Hazard ratio (95% CI)	P value	Hazard ratio (95% CI)	P value	Hazard ratio (95% CI)	P value	Hazard ratio (95% CI)	P value
Gender								
Male	Reference				Reference			
Female	1.028 (0.542-1.950)	0.934			1.101 (0.581-2.087)	0.768		
Age (years)	1.001 (0.976-1.027)	0.919			0.999 (0.975-1.024)	0.957		
Hepatitis status								
HBV	Reference				Reference			
HCV	1.058 (0.331-3.382)	0.924			1.163 (0.365-3.712)	0.798		
Other	0.860 (0.428-1.729)	0.672			0.894 (0.445-1.796)	0.753		
Cirrhosis								
Yes	Reference				Reference			
No	0.837 (0.532-1.317)	0.441			0.942 (0.598-1.483)	0.795		
Tumor necrosis								
Yes	Reference				Reference		Reference	
No	0.645 (0.409-1.018)	0.060			0.574 (0.364-0.906)	0.017	0.822 (0.497-1.360)	0.446
Microvascular infiltration								
MO	Reference		Reference		Reference		Reference	
M1	2.389 (1.384-4.126)	0.002	2.987 (1.698-5.256)	< 0.001	2.352 (1.376-4.020)	0.002	2.480 (1.431-4.299)	0.001
M2	6.437 (3.465-11.960)	< 0.001	4.824 (2.542-9.157)	< 0.001	5.405 (2.986-9.782)	< 0.001	3.703 (1.929-7.109)	< 0.001
ALT (U/L)	1.001 (0.999-1.002)	0.298			1.001 (0.999-1.002)	0.317		

AST (U/L)	0.997 (0.992-1.003)	0.343			0.997 (0.991-1.003)	0.312		
AFP (ng/mL)								
<400	Reference		Reference		Reference		Reference	
≥ 400	4.900 (2.935-8.181)	< 0.001	3.291 (1.933-5.603)	< 0.001	4.974 (3.004-8.235)	< 0.001	2.972 (1.744-5.065)	< 0.001
Number of tumors								
Unifocal	Reference				Reference			
Multifocal	1.443 (0.866-2.402)	0.159			1.328 (0.797-2.211)	0.276		
Maximum tumor size (cm)								
< 3	Reference				Reference			
3-5	1.566 (0.868-2.826)	0.137			1.448 (0.803-2.609)	0.218		
> 5	1.741 (0.949-3.195)	0.073			1.509 (0.825-2.761)	0.182		
Child-pugh Class								
A	Reference				Reference			
В	1.061 (0.147-7.650)	0.953			1.119 (0.155-8.078)	0.911		
BCLC stage								
A	Reference				Reference			
В	0.690 (0.299-1.593)	0.385			0.645 (0.279-1.491)	0.305		
H-Score	1.021 (1.015-1.028)	< 0.001	1.022 (1.015-1.028)	< 0.001	1.021 (1.015-1.027)	< 0.001	1.020 (1.015-1.026)	< 0.001

Abbreviations: AFP, alpha-fetoprotein; ALT, alanine aminotransferase; AST, aspartate aminotransferase; BCLC, Barcelona Clinic Liver Cancer; HBV, Hepatitis B Virus; HCV, Hepatitis C Virus; TACE, transarterial chemoembolization.

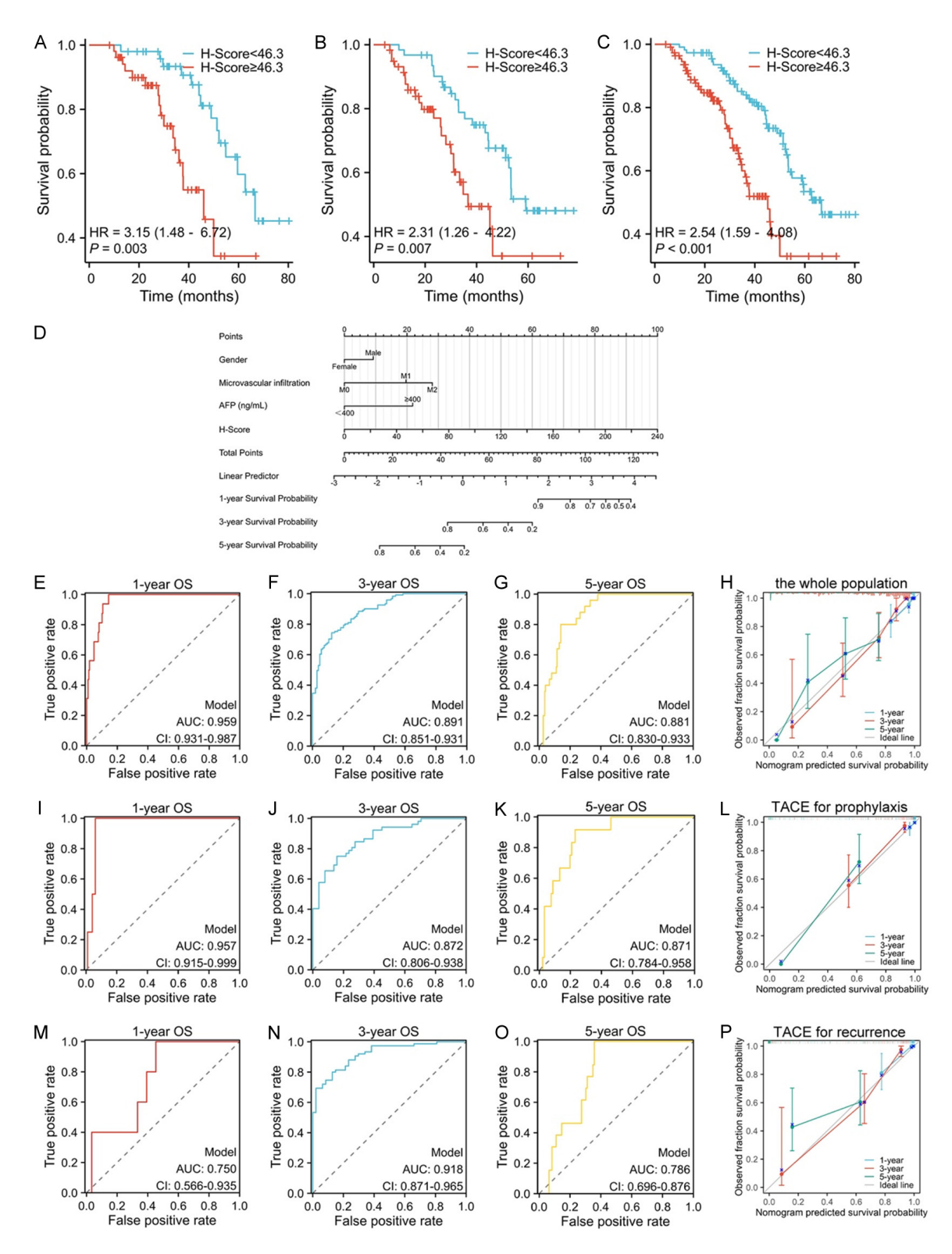
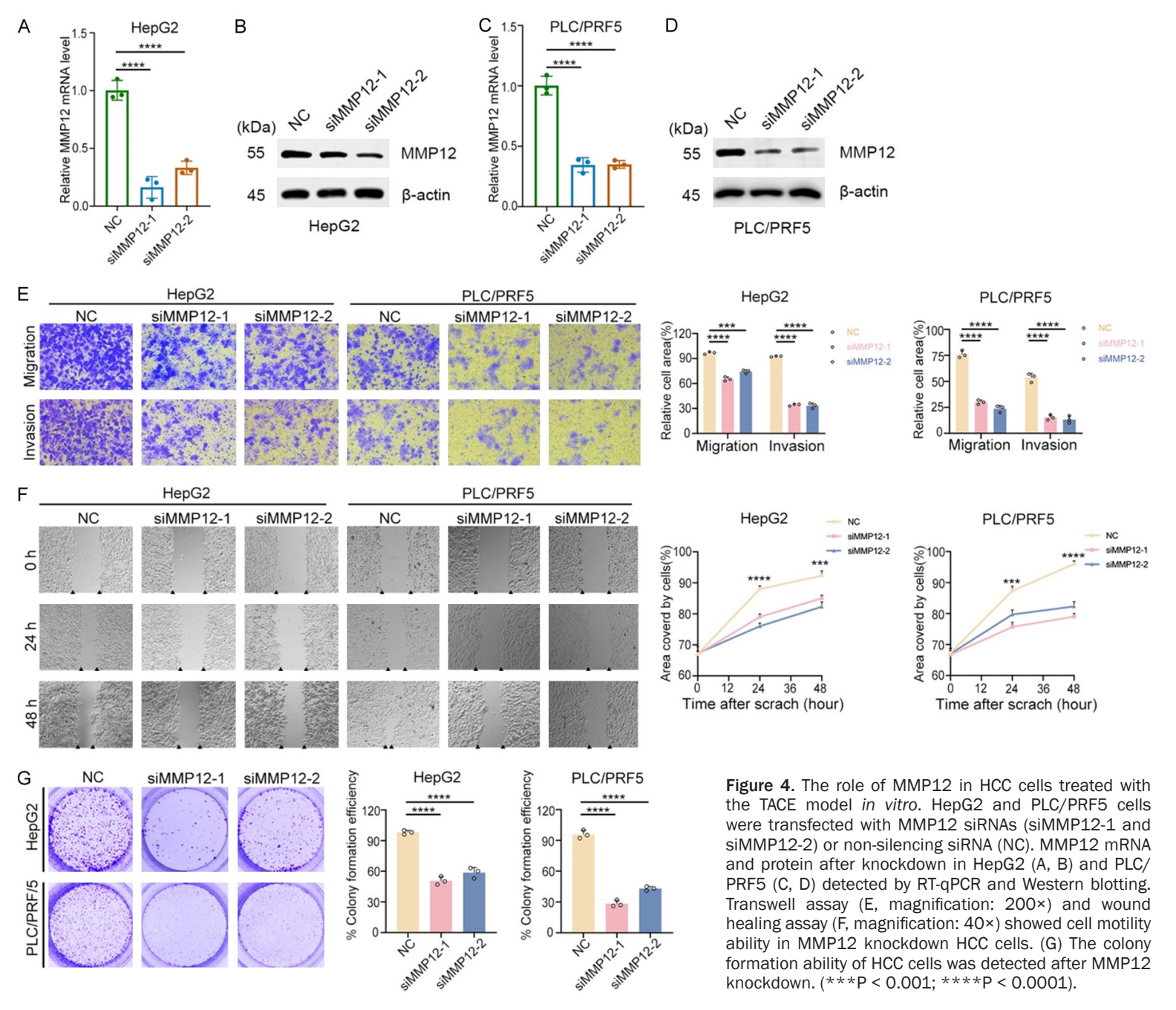


Figure 3. Predictive value of MMP12 for OS in PA-TACE patients. Kaplan-Meier curves for OS of the H-score < 46.3 and H-score \ge 46.3 groups in the TACE group for prophylaxis (A) and TACE group for recurrence (B) and in the whole population (C). (D) Nomogram of the predictive model for the whole population OS. ROC curves to evaluate the accuracy of the prediction model based on the overall population (E-G), the TACE group for prophylaxis (I-K) and the TACE group for recurrence (M-O). Calibration plots to assess the calibration of the prediction model based on the overall population (H), the TACE group for prophylaxis (L) and the TACE group for recurrence (P).



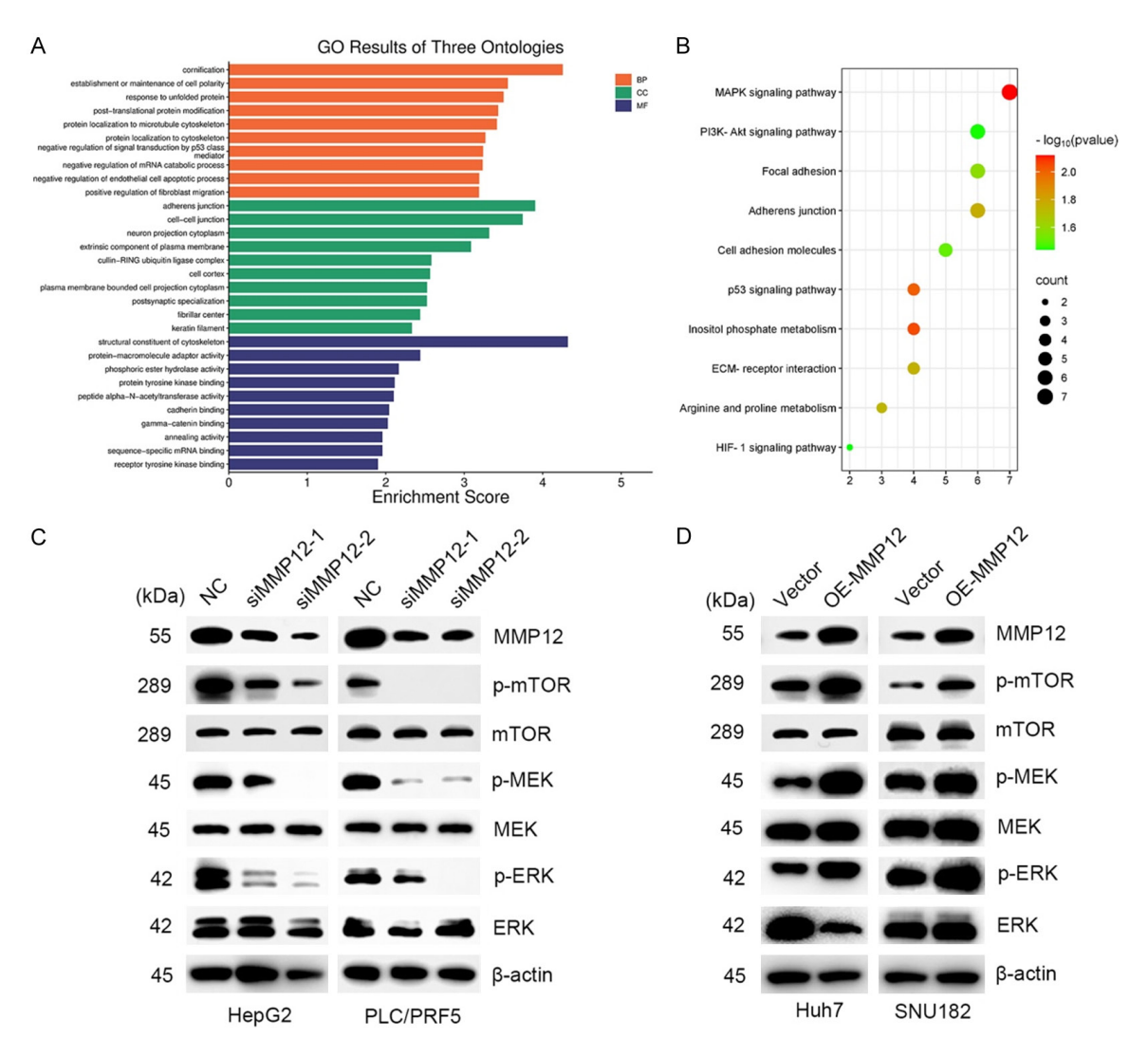


Figure 5. MMP12 activated MEK/ERK signaling pathway. Mass spectrometry detection was performed on the cells after MMP12 knockdown. KEGG (A) and GO (B) analyses showed the signaling pathways and biological functions analyses regulated by MMP12. (C, D) Western blotting results showed that MMP12 activated MEK/ERK signaling pathway.

were independent risk factors for OS in the overall cohort (**Table 4**).

Based on the multivariate analysis of all patients, a nomogram was constructed (Figure 3D), and its predictive performance was evaluated using ROC curves and calibration plots. The ROC curves showed AUC values of 0.959, 0.891, and 0.881, indicating that the model achieved strong predictive accuracy across all three time points (1, 3 and 5 year) (Figure 3E-G). Calibration analysis demonstrated good agreement between predicted and observed outcomes (Figure 3H). To verify the stability of the model, we analyzed the prognostic model derived from the cohort in two subgroups: TACE for the prophylaxis group and TACE for

the recurrence group. The results showed that the AUC values for the prophylaxis group were 0.957, 0.872, and 0.871 at 1, 3, and 5 years, respectively (**Figure 3I-K**). The AUC values of the recurrence group at the corresponding time points were 0.750, 0.918, and 0.786, respectively (**Figure 3M-O**). In additionally, the calibration curves showed satisfactory outcomes (**Figure 3L, 3P**).

Knockdown of MMP12 inhibited the migration, invasion, wound healing and colony formation of HCC cells

To investigate the role of MMP12 in TACE-treated HCC, functional studies were perfor-

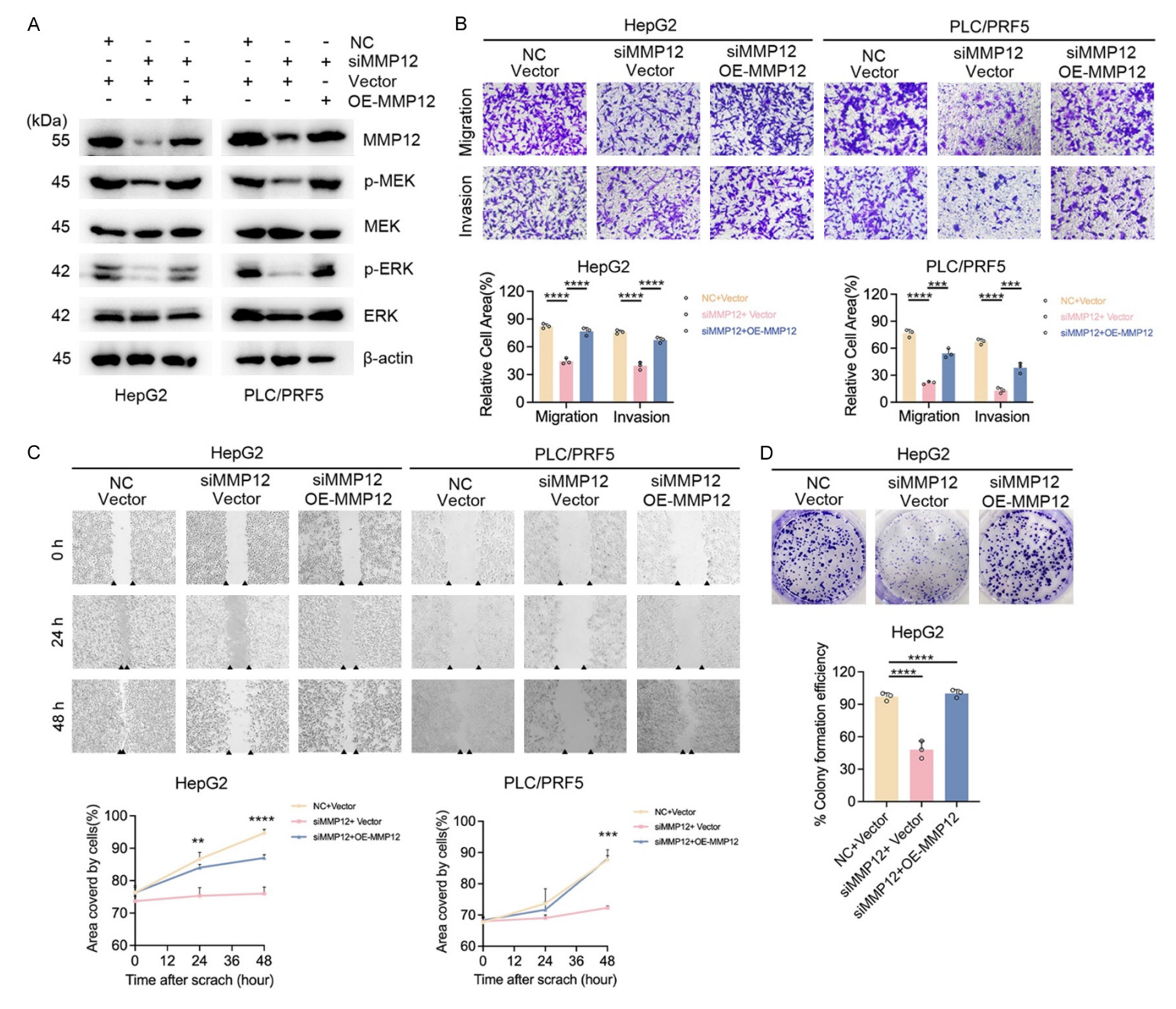


Figure 6. MMP12 specifically regulated the response of cells to TACE. (A) Western blotting was used to detect protein levels after knockdown of MMP12 and transfection with the overexpression vectors of MMP12 in HepG2 and PLC/PRF5 cells. Transwell assay (B, magnification: 200×) and wound healing assay (C, magnification: 40×) showed cell motility abilities in HepG2 and PLC/PRF5 cells with MMP12 knockdown and subsequently transfected with MMP12 overexpression vector. (D) The colony formation ability of HCC cells was detected after MMP12 knockdown and the reintroduction of MMP12 overexpression vector (**P < 0.01; ****P < 0.001; ****P < 0.0001). Vector: pCMV-MCS-3×Flag, OE-MMP12: pCMV-MCS-MMP12-3×Flag.

med using HepG2 and PLC/PRF5 cell lines with high MMP12 expression. An in vitro TACE model was established using 0.2 µM Dox combined with 1% 0₂. MMP12 was knocked down using MMP12 siRNAs (siMMP12-1 and siMMP12-2) and a control siRNA (NC). RT-gPCR and Western blotting showed that MMP12 mRNA and protein levels were significantly reduced in the siMMP12-1 and siMMP12-2 groups compared with the negative control group (Figure 4A-D). The migration assay showed that compared to the negative control group, the number of migrated cells was significantly lower in the si-MMP12-1 and siMMP12-2 groups (Figure 4E). Similarly, in the invasion assay, the number of invaded cells was significantly decreased in the siMMP12-1 and siMMP12-2 groups (Figure **4E**), further confirming that MMP12 knockdown inhibited cell invasion. In the wound healing assay, the scratch closure rate in the siMMP-12-1 and siMMP12-2 groups were significantly reduced indicating that MMP12 knockdown decreased the wound healing ability of HCC cells (Figure 4F), suggesting that MMP12 knockdown effectively suppressed cell migration. Additionally, the colony formation assay revealed that the number of colonies formed was significantly reduced in the siMMP12-1 and siMMP12-2 groups, indicating that MMP12 knockdown suppressed the cells' proliferative capacity (Figure 4G).

MMP12 activates MEK/ERK signaling pathway

To investigate the potential relationship between MMP12 expression, the response of HCC cells to TACE, and the clinical outcomes of patients with HCC receiving TACE, MMP12 was downregulated in HepG2 and PLC/PRF5 cell lines under conditions mimicking TACE (0.2 μ M Dox and 1% $\rm O_2$). Subsequently, protein mass spectrometry was performed on cells with MMP12 knockdown and on non-silencing controls. GO enrichment analysis was used to predict the effects of MMP12 on molecular functions, cellular components, and biological processes in HCC. The results revealed that

most of the molecules involved were associated with adherens junctions, cell-cell junctions. and extrinsic components of the plasma membrane (Figure 5A). Furthermore, KEGG pathway analysis indicated that MMP12 was linked to the MAPK signaling pathway (Figure 5B). Western blotting showed that the phosphorylation levels of MEK and ERK were reduced after MMP12 knockdown in HepG2 and PLC/PRF5 cells; however, total MEK and ERK protein levels remained unchanged (Figure 5C). Conversely, MEK and ERK phosphorylation levels increased after MMP12 overexpression in Huh7 and SNU182 cells, while total MEK and ERK levels remained unchanged (Figure 5D), indicating that MMP12 activated the MEK/ERK signaling pathway. This finding is consistent with the KEGG pathway enrichment results.

MMP12 promotes the malignant phenotype of HCC cells through activating MEK/ERK signaling pathway

To confirm the role and specificity of targeting MMP12 in enhancing the therapeutic effect of Dox under the in vitro TACE model conditions. we utilized siRNA-mediated MMP12 knockdown in HepG2 and PLC/PRF5 cell lines, and then reintroduced MMP12 through overexpression vectors to perform rescue experiments. The Western blotting results showed that after knocking down MMP12, the phosphorylation levels of MEK and ERK decreased, while after further transfecting with the MMP12 overexpression plasmid, the activities of MEK and ERK significantly increased (Figure 6A). The phenotypic experimental results indicated that knockdown of MMP12 significantly reduced the migration, invasion and wound healing abilities of HepG2 and PLC/PRF5 cells. In contrast, overexpression of MMP12 rescued these phenotypes and restored the migration, invasion and wound healing abilities of the cells (Figure 6B, 6C). In addition, the colony formation experiment showed that the number of colonies formed by MMP12 knockdown cells decreased significantly, while the number of colonies

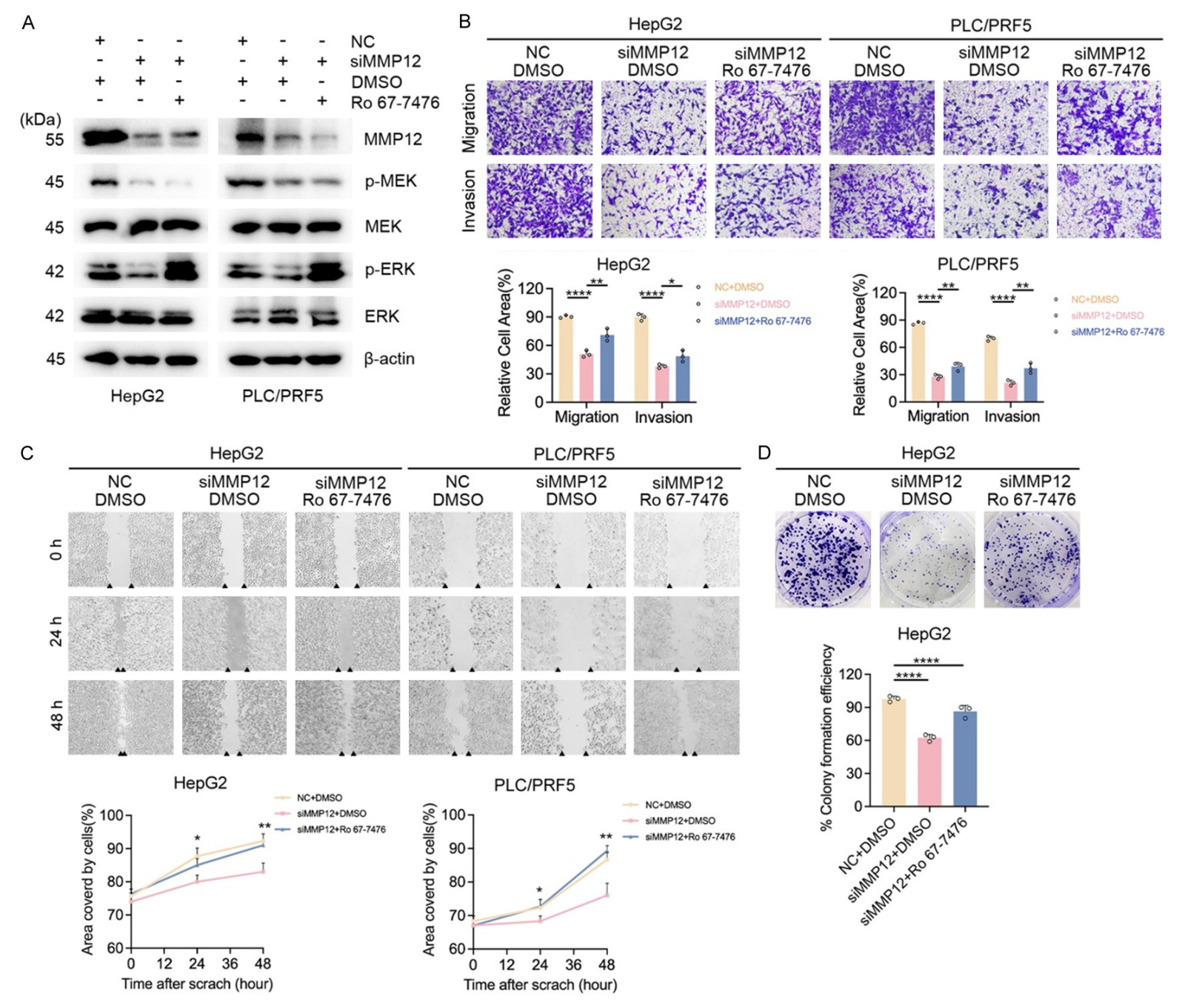


Figure 7. Effect of MMP12 knockdown and restoration of MEK/ERK signaling activity. (A) Western blotting was used to detect protein levels after knockdown of MMP12 and subsequent treatment with MEK/ERK activator Ro 67-7476 in HepG2 and PLC/PRF5 cells. The Transwell assay (B, magnification: 200×) and wound healing assay (C, magnification: 40×) showed cell motility abilities in HepG2 and PLC/PRF5 cells with MMP12 knockdown and subsequent treatment with Ro 67-7476. (D) The colony formation ability of HCC cells was detected after MMP12 knockdown and subsequent treatment with Ro 67-7476 (**P < 0.01; ***P < 0.001; ****P < 0.0001).

increased after MMP12 overexpression was rescued (**Figure 6D**). These results provide evidence that MMP12 specifically regulates the response of cells to TACE.

We then performed rescue experiments by altering MEK/ERK activity. In MMP12 knockdown HepG2 and PLC/PRF5 cells, we treated the cells with the ERK activator Ro 67-7476 (1 μM) to restore MEK/ERK signaling. Conversely, in Huh7 and SNU182 cells overexpressing MMP12, we used the MEK inhibitor trametinib (1 μM) and the ERK inhibitor SCH772984 (1 µM), respectively, to inhibit the MEK/ERK pathway. Western blotting analysis confirmed that the treatment with Ro 67-7476 in MMP12 knockdown cells significantly restored the phosphorylation levels of ERK, indicating successful reactivation of the MEK/ERK signaling pathway (Figure 7A). We then evaluated the restoration of migration and invasion activities of the cells under TACE conditions. The results of transwell and wound healing assays showed that in MMP12 knockdown HepG2 and PLC/ PRF5 cells, treatment with Ro 67-7476 significantly rescued the migration and invasion activities (Figure 7B, 7C), indicating that the reactivation of the MEK/ERK pathway could restore the migration and invasion phenotypes. The colony formation assay results showed that in MMP12 knockdown HepG2 cells, treatment with Ro 67-7476 significantly increased the number of colonies formed, rescuing the reduced colony formation ability (Figure 7D).

Similarly, in MMP12 overexpressing Huh7 and SNU182 cells, treatment with trametinib or SCH772984 effectively reduced the phosphorylation levels of MEK and ERK (Figures 8A and 9A), confirming the successful inhibition of the pathway. The treatment with either trametinib or SCH772984 in MMP12 overexpressing cells significantly attenuated the enhanced migration and invasion activities (Figures 8B, 8C and 9B, 9C) and also decreased the number of colonies (Figures 8D and 9D).

These findings provide evidence that MMP12 regulates HCC cell response to TACE, at least in part, through the MEK/ERK signaling pathway. The rescue experiments clearly demonstrate the functional relevance of the MEK/ERK pathway in mediating the effects of MMP12 on HCC cell motility.

The small molecule inhibitor of MMP12 significantly enhanced the effect of TACE

Currently, several inhibitors directly targeting MMP12 are under investigation for clinical applications, including GM6001 (also known as ilomastat), which directly targets MMP12. GM6001 inhibits MMP12 at its active site, thereby preventing the breakdown of the extracellular matrix and its subsequent effects on cell behavior and tissue integrity [35]. This study aims to explore whether the combined effect of GM6001 and Dox can also be extended to inhibit the migration, invasion and colony formation of HCC cells. To verify this, a transwell assay was performed, where HepG2 and PLC/PRF5 cells were treated in combination with 10 μ M GM6001 and 0.2 μ M Dox. The results indicated that in both cell lines, the combined treatment significantly enhanced the inhibitory effect on cell migration and invasion compared with the use of 10 µM GM6001 or 0.2 µM Dox alone (Figure 10A). To evaluate the impact of combined treatment on cell migration, a wound healing assay was conducted after treatment, enabling us to determine the migration abilities of HCC cells. The results indicated that the combined treatment was more effective in inhibiting cell migration than either GM6001 or Dox alone (Figure 10B). In addition, the colony formation assay revealed that the combined treatment significantly reduced the number of colonies (Figure 10C). These findings suggest that the combined treatment of GM6001 and Dox may offer a more effective strategy for inhibiting the metastatic potential of HCC cells.

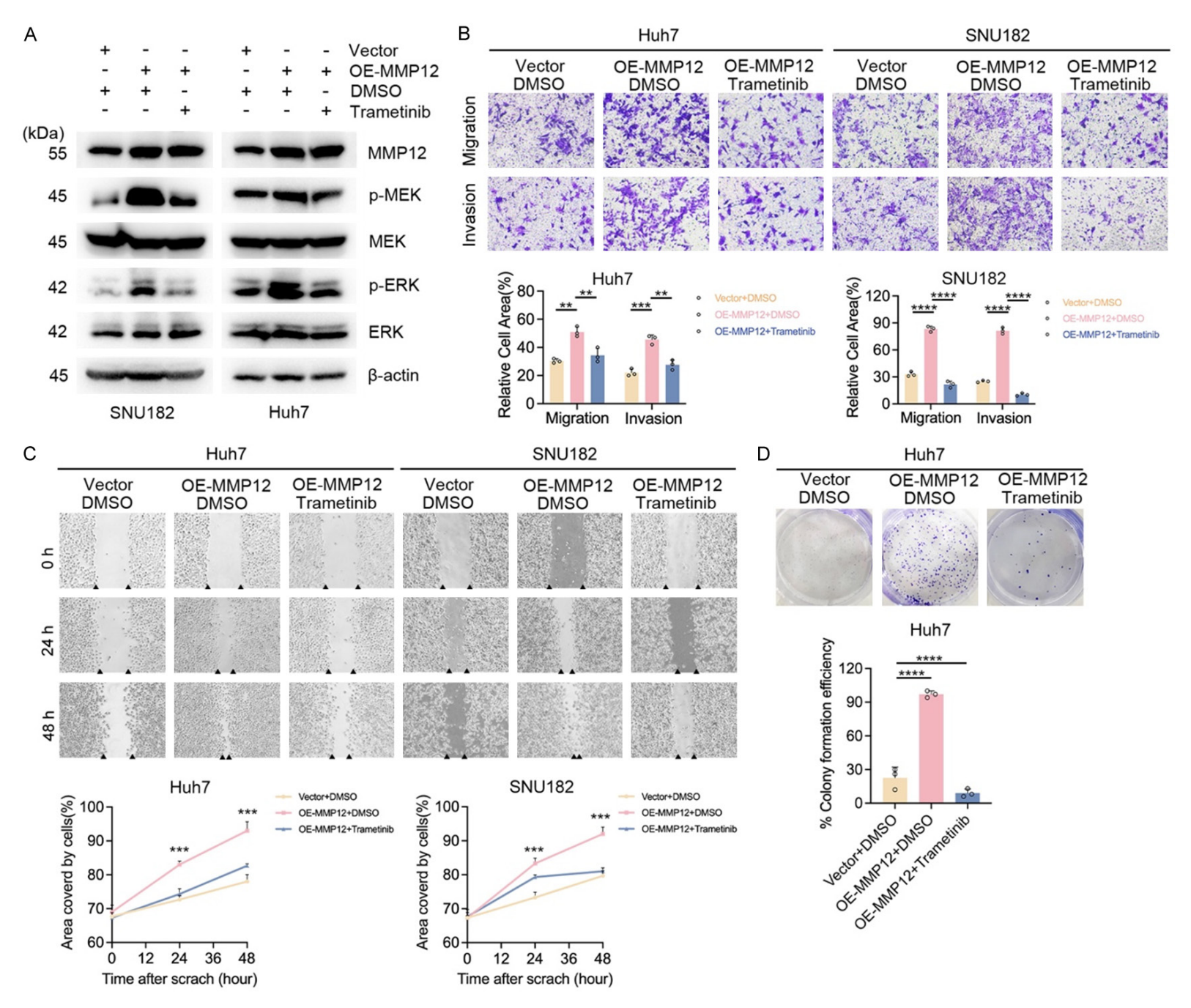


Figure 8. Effect of MMP12 overexpression and subsequent inhibition of MEK activity. (A) Western blotting was used to detect protein levels after the overexpression of MMP12 and subsequent treatment with MEK inhibitor trametinib in Huh7 and SNU182 cells. The Transwell assay (B, magnification: $200\times$) and wound healing assay (C, magnification: $40\times$) showed cell motility abilities in Huh7 and SNU182 cells with MMP12 overexpression and subsequent treatment with trametinib. (D) The colony-formation ability of HCC cells was detected after MMP12 overexpression and subsequent treatment with trametinib (**P < 0.01; ***P < 0.001; ****P < 0.0001).

Discussion

Postoperative neoplasm recurrence significantly contributes to the increased mortality rate in patients with HCC [36], and PA-TACE has demonstrated effectiveness in the treatment of HCC. However, relatively few studies have investigated the prognosis and risk factors for recurrence [37-39]. Several studies have developed models to predict the prognosis of patients with HCC following PA-TACE. A nomogram for estimating the disease outcomes of patients receiving PA-TACE for HCC was previously published by Hu et al., in which 235 patients were enrolled, and the nomogram's C-index was 0.75 (95% CI: 0.67-0.83). However, this study was limited to patients with HBVrelated HCC [40].

In 2023, Wu et al. published a study on the impact of PA-TACE on the clinical outcomes of patients with HCC. They reported that liver cirrhosis, maximum tumor diameter, vascular invasion (imaging), Child-Pugh classification, microvascular invasion (MVI), satellite nodules, differentiation grade, adjuvant TACE, lymphocyte-to-monocyte ratio, and CNLC staging were independent predictors of OS. However, they did not stratify the population that received adjuvant TACE either prophylactically or after relapse [41]. Other studies have shown similar limitations [42-44].

In the present study, we used immunohistochemistry to detect and analyze MMP12 protein levels in tumor tissues from 255 HCC patients who underwent radical resection. To evaluate the expression levels of MMP12, we employed the H-score, a widely used semiquantitative method that integrates both the percentage of positive cells and the intensity of staining. This method has been adopted by many studies due to its reliability and standardization [27-29]. The advantage of H-score is that it reduces subjectivity, improves the reproducibility and comparability of results, and thus provides more accurate quantitative analysis. By using H-score, we were able to objectively

compare MMP12 expression in different samples, which laid the foundation for our subsequent analysis and conclusions. We identified MMP12 as a novel prognostic biomarker for PA-TACE and found that MMP12, AFP, and MVI status were independently associated with unfavourable outcomes. Our findings indicate that MMP12 has an independent predictive effect on OS and PFS following PA-TACE, whether in the TACE group for prophylaxis, the TACE group for recurrence, or in the overall HCC population. A previous study detected elevated levels of MMP12 mRNA in the tumor tissues of HCC patients and reported that high MMP12 expression was significantly associated with venous invasion, elevated AFP levels, early tumor recurrence, and poorer OS [20], supporting the reliability of our findings. Based on these results, we developed a new predictive model to more accurately estimate OS and PFS in patients following PA-TACE. This model incorporated multiple key indicators and employed calibration and decision curve analyses to evaluate the predictive performance of the nomogram. According to the ROC curves, the AUC values for all three time points in predicting OS and PFS were greater than 0.85, demonstrating that our model has strong predictive accuracy and discriminatory power.

The aim of this study was to identify key factors influencing the clinical outcomes of patients with HCC receiving adjuvant TACE therapy following hepatectomy. Unlike previous studies, which primarily focused on patients with postoperative high-risk indicators for recurrence or those receiving TACE after recurrence, our study included two subgroups: patients receiving prophylactic TACE after surgery and patients receiving TACE after tumor recurrence. By conducting Cox regression analyses in these two groups, we aimed to identify independent risk factors for PFS and OS and assess the reliability of these factors. In addition, we combined the two groups into a single cohort and analyzed the entire population. Notably, the independent risk factors identified in the overall

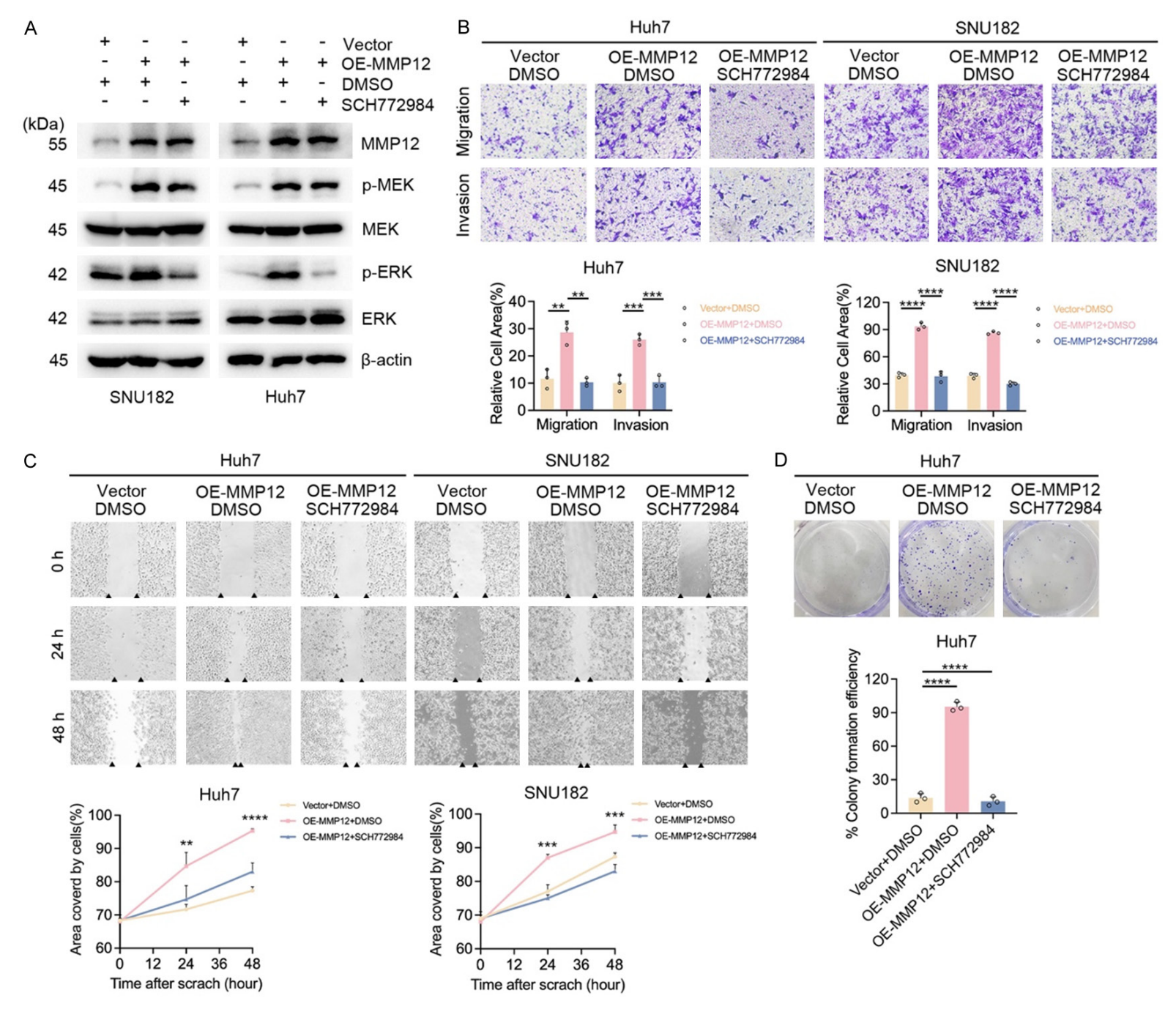


Figure 9. Effect of MMP12 overexpression and subsequent inhibition of ERK activity. (A) Western blotting was used to detect protein levels after the overexpression of MMP12 and subsequent treatment with ERK inhibitor SCH772984 in Huh7 and SNU182 cells. (B) The Transwell assay (B, magnification: $200\times$) and wound healing assay (C, magnification: $40\times$) showed cell motility abilities in Huh7 and SNU182 with MMP12 overexpression and subsequent treatment with SCH772984. (D) The colony formation ability of HCC cells was detected after MMP12 overexpression and subsequent treatment with SCH772984 (**P < 0.01; ***P < 0.001; ****P < 0.0001).

population were consistent with the common factors derived from analyses of the two subgroups. This finding not only validates the reliability of the subgroup analysis results but also provides a solid foundation for constructing prognostic models. The high-performance prognostic model developed in this study may help identify HCC patients who are suitable for and likely to benefit from PA-TACE therapy, thereby improving patient stratification and informing clinical decision-making.

MMP12 is a key mediator of extracellular matrix remodeling that affects cell migration, invasion, angiogenesis, and proliferation [45, 46]. However, it is rarely considered when evaluating which patients may experience improved outcomes following PA-TACE treatment. Previous studies have suggested that rapid progression of HCC after surgery may be due to the presence of occult micrometastases in previously highly proliferative and invasive primary tumors [47-49]. Similar to disseminated tumor cells (DTCs) in the bloodstream, HCC with high MMP12 expression may have strong migratory and invasive potential. If primary tumor cells produce high levels of MMP12, it is possible that the tumor cells disseminated through the bloodstream are phenotypically similar to the original tumor cells. High migration and invasion potential DTCs preserve the homogeneity of the original tumor when they settle in the remanent liver or metastasize to distant sites such as the lung, brain, or bone, leading to early disease progression and a worse prognosis. MMP12 carried substantial weight in our model, which is consistent with its role as a typical variable associated with tumor migration and invasion.

We further validated the role and underlying mechanisms of MMP12 overexpression at the cellular level by conducting wound healing, migration, invasion, and colony formation assays. We found that MMP12 affected the malignant biological behavior of tumor cells under conditions of $1\%~\rm O_2$ and $0.2~\mu M$ Dox, mimicking TACE, thereby further confirming the correlation

between MMP12 expression and both the response of HCC cells to TACE and the prognosis of patients treated with TACE. Because chemotherapeutic drugs such as Dox are used in TACE, we speculated that MMP12 expression is associated with tumor cell susceptibility to chemotherapy. Indeed, inhibiting MMP12 enhanced the efficacy of TACE. In in vitro TACE experiments, we found that the MMP12 inhibitor GM6001 increased the sensitivity of HCC cell lines to Dox. Although GM6001 is a broadspectrum MMP inhibitor, we used siRNA-mediated knockdown and overexpression of MMP12 to demonstrate its specific role in HCC cells. The results of these experiments showed that MMP12 knockdown significantly reduced cell migration, invasion, and colony formation, and these effects were rescued by MMP12 overexpression. These findings provide strong evidence that the observed effects on cell behavior are attributable to MMP12 rather than off-target effects on other MMPs. Moreover, these findings further support the association between MMP12 expression and the response to TACE. However, the precise mechanisms through which MMP12 influences chemotherapeutic drug sensitivity require further investigation.

Based on KEGG signaling pathway analysis, we observed a strong correlation between MMP12 expression and activation of the MAPK signaling pathway under in vitro TACE conditions, indicating that MMP12 may participate in malignant HCC-related activities through this pathway, thereby affecting the response of HCC cells to TACE. The MEK/ERK signaling pathway is a crucial intracellular signal transduction pathway that regulates cell differentiation and survival [50, 51]. Previous studies have demonstrated that MMP12 regulates the proliferation of mouse macrophages and the secretion of inflammatory cytokines, including IL-1β, IL-6, and CXCL3, during the inflammatory process via the ERK/MAPK pathway [52]. These findings suggest that MMP12 influences cell behavior by modulating the MEK/ERK signaling

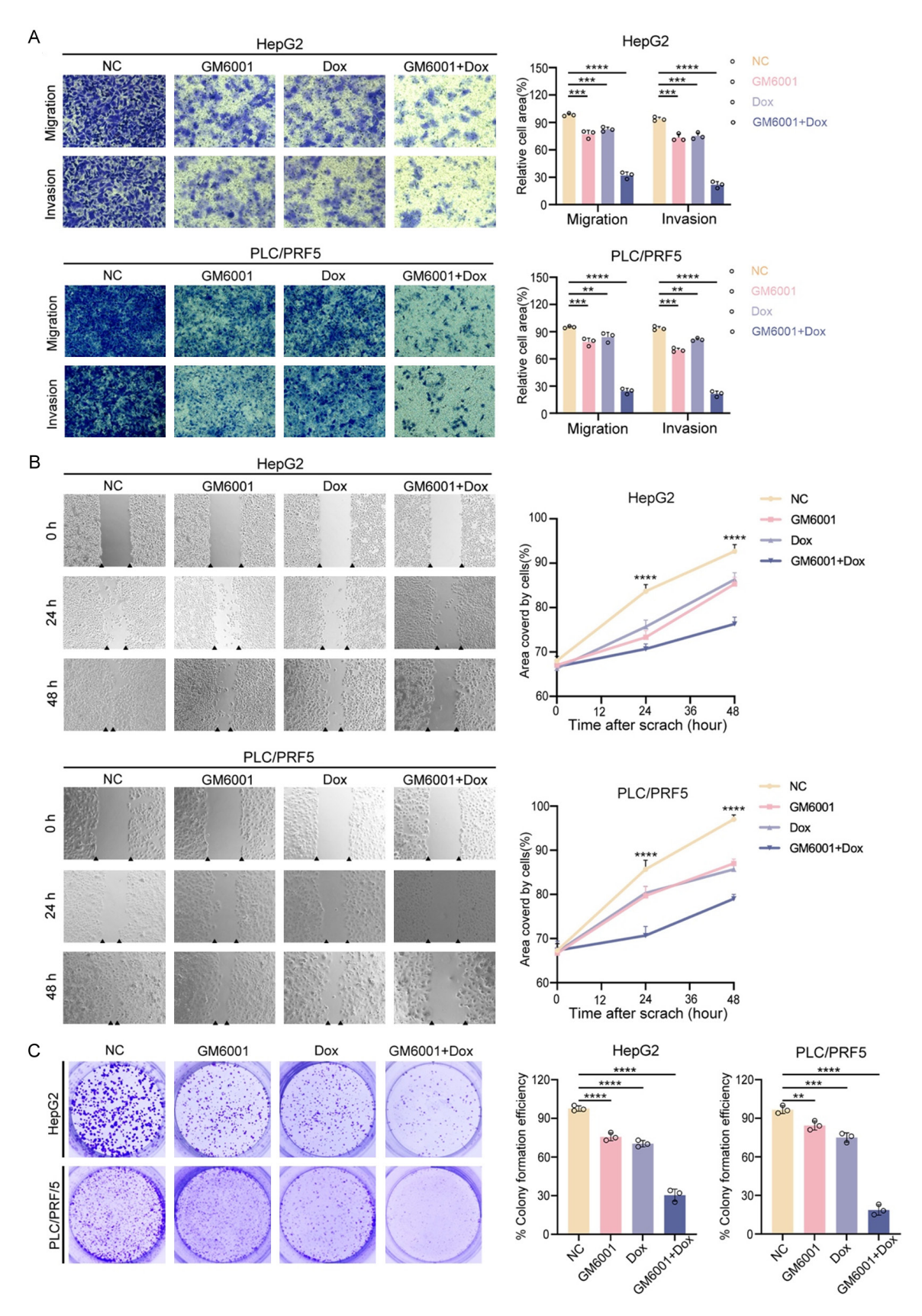


Figure 10. GM6001 enhances the ability of Dox to inhibit the migration, invasion, and colony formation of HCC cells under 1% 0, conditions. The effects of GM6001, Dox alone or in combination therapy on the motility ability

of HepG2 and PLC/PRF5 cells were assessed by the Transwell assay (A, magnification: $200\times$) and wound healing assay (B, magnification: $40\times$). (C) Colony formation of HepG2 and PLC/PRF5 cells exposed to single drug or combination therapy. (**P < 0.01; ***P < 0.001; ****P < 0.001).

pathway, thereby affecting cell proliferation and inflammatory responses within the tumor microenvironment. Consistent with the existing literature and KEGG pathway analysis, we propose that MMP12 mediates MEK/ERK signaling in HCC cells, leading to enhanced cell migration, invasion, and drug resistance.

Our Western blotting results confirmed that MMP12 knockdown inhibited the MEK/ERK signaling pathway, whereas MMP12 overexpression enhanced its activation. To ensure the rigor of our findings, we conducted rescue experiments in cells with MMP12 knockdown or overexpression using the p-ERK activator Ro 67-7476, the MEK inhibitor trametinib, and the ERK inhibitor SCH772984. The results of these rescue experiments further clarified the regulatory role of MMP12 in the MEK/ERK signaling pathway. These findings indicate that MMP12 enhances the migratory capacity and drug resistance of HCC cells by upregulating the MEK/ ERK signaling pathway, thereby influencing the efficacy of TACE to a certain extent.

Taken together, this study not only established an effective prognostic model but also identified MMP12 as a key factor influencing the clinical outcomes of patients with HCC following PA-TACE at the molecular level. Furthermore, we confirmed at the cellular level the correlation between MMP12 expression and TACE responses through MMP12 inhibition and gene knockdown experiments, providing a new perspective and a scientific basis for personalized HCC treatment. Our results suggest that, for HCC patients with high MMP12 expression in tumor tissues, targeting MMP12 has the potential to improve the therapeutic efficacy of PA-TACE.

Although our nomogram performed well, this study has several limitations. First, it was a single-center, retrospective study with a relatively small sample size, which may have introduced selection bias and limited the generalizability of our findings. Future studies should aim to increase the sample size and involve multiple centers to enhance the robustness and applicability of the model. Second, we were unable

to perform p-ERK or p-MEK IHC staining on clinical samples due to limitations in sample preservation at the time of collection. This prevented us from directly correlating MEK/ERK pathway activity with MMP12 levels in tumors. We plan to prioritize this analysis in future experiments to further validate our findings. Lastly, it should be noted that since all patients in this study received TACE treatment and there was a lack of a control group that did not receive TACE treatment, our current results can only confirm that MMP12 is a strong prognostic factor for the patient group that received TACE treatment. To ultimately confirm MMP12 as a specific predictive marker for the efficacy of TACE, validation still needs to be conducted in the following models: 1) Randomized controlled trials or prospective cohort studies involving patients who received TACE treatment and those who did not; 2) The role and underlying mechanism of MMP12 under simulated TACE and non-TACE conditions should be compared and studied in vitro and in vivo experiments. In addition, clinical trials are warranted to verify whether targeting MMP12 with its inhibitor can improve the survival of HCC patients undergoing PA-TACE therapy.

Conclusion

The present study identified an important prognostic biomarker for patients with HCC undergoing PA-TACE. We established a novel and effective prognostic model combining MMP12, AFP, and MVI, which may help identify HCC patients who are suitable for and likely to benefit from PA-TACE therapy. Knockdown of MMP12 inhibited cell migration, invasion, and colony formation in HCC cells by suppressing the MEK/ERK signaling pathway. In addition, a small-molecule inhibitor of MMP12 significantly enhanced the efficacy of TACE, suggesting that MMP12 has potential as a therapeutic target to improve the effectiveness of PA-TACE in HCC patients with high MMP12 expression.

Acknowledgements

This work was supported and funded by the National Natural Science Foundation of China

(82330061), The Science and Education Cultivation Fund of the National Cancer and Regional Medical Center of Shanxi Provincial Cancer Hospital (grant No: TD2023003) and Chinese Academy of Medical Sciences (CAMS) Innovation Fund for Medical Sciences (CIFMS, 2023-I2M-2-004).

Disclosure of conflict of interest

None.

Address correspondence to: Xiao Li, Department of Interventional Therapy, National Cancer Center/ National Clinical Research Center for Cancer/Cancer Hospital, Chinese Academy of Medical Sciences and Peking Union Medical College, Beijing 100021, P. R. China. E-mail: simonlixiao@263.net; Jia-Jie Hao, State Key Laboratory of Molecular Oncology, Center for Cancer Precision Medicine, National Cancer Center/National Clinical Research Center for Cancer/Cancer Hospital, Chinese Academy of Medical Sciences and Peking Union Medical College, Beijing 100021, P. R. China. E-mail: haojiajie@cicams.ac.cn

References

- [1] Chan SL, Wong VW, Qin S and Chan HL. Infection and cancer: the case of hepatitis B. J Clin Oncol 2016; 34: 83-90.
- [2] Dhanasekaran R, Nault JC, Roberts LR and Zucman-Rossi J. Genomic medicine and implications for hepatocellular carcinoma prevention and therapy. Gastroenterology 2019; 156: 492-509.
- [3] Torimura T and Iwamoto H. Treatment and the prognosis of hepatocellular carcinoma in Asia. Liver Int 2022; 42: 2042-2054.
- [4] Gomaa AI and Waked I. Recent advances in multidisciplinary management of hepatocellular carcinoma. World J Hepatol 2015; 7: 673-687.
- [5] Bruix J and Llovet JM. Prognostic prediction and treatment strategy in hepatocellular carcinoma. Hepatology 2002; 35: 519-524.
- [6] Bruix J, Gores GJ and Mazzaferro V. Hepatocellular carcinoma: clinical frontiers and perspectives. Gut 2014; 63: 844-855.
- [7] Fukumoto T, Tominaga M, Kido M, Takebe A, Tanaka M, Kuramitsu K, Matsumoto I, Ajiki T and Ku Y. Long-term outcomes and prognostic factors with reductive hepatectomy and sequential percutaneous isolated hepatic perfusion for multiple bilobar hepatocellular carcinoma. Ann Surg Oncol 2014; 21: 971-978.
- [8] Zuo CH, Xia M, Liu JS, Qiu XX, Lei X, Xu RC, Liu HC, Li JL, Li YG, Li QL, Xiao H, Hong Y, Wang XH,

- Zhu HZ, Wu QF, Burns M and Liu C. Transcatheter arterial chemoembolization combined with interferon-alpha is safe and effective for patients with hepatocellular carcinoma after curative resection. Asian Pac J Cancer Prev 2015; 16: 245-251.
- [9] Bruix J and Sherman M; Practice Guidelines Committee, American Association for the Study of Liver Diseases. Management of hepatocellular carcinoma. Hepatology 2005; 42: 1208-1236.
- [10] Feng AL, Zhu JK, Yang Y, Wang YD, Liu FY, Zhu M and Liu CZ. Repeated postoperative adjuvant TACE after curative hepatectomy improves outcomes of patients with HCC. Minim Invasive Ther Allied Technol 2019; 30: 163-168.
- [11] Zhong JH and Li LQ. Postoperative adjuvant transarterial chemoembolization for participants with hepatocellular carcinoma: a metaanalysis. Hepatol Res 2010; 40: 943-953.
- [12] Jiang JH, Guo Z, Lu HF, Wang XB, Yang HJ, Yang FQ, Bao SY, Zhong JH, Li LQ, Yang RR and Xiang BD. Adjuvant transarterial chemoembolization after curative resection of hepatocellular carcinoma: propensity score analysis. World J Gastroenterol 2015; 21: 4627-4634.
- [13] Gu J, Zhang X, Cui R, Zhang J, Wang Z, Jia Y, Miao R, Dong Y, Ma X, Fan H, Wang H, Ren L, Li Y, Niu W, Zhang J, Qu K and Liu C. Prognostic predictors for patients with hepatocellular carcinoma receiving adjuvant transcatheter arterial chemoembolization. Eur J Gastroenterol Hepatol 2019; 31: 836-844.
- [14] Qiu Y, Yang Y, Wang T, Shen S and Wang W. Efficacy of postoperative adjuvant transcatheter arterial chemoembolization in hepatocellular carcinoma patients with microscopic portal vein invasion. Front Oncol 2022; 12: 831614.
- [15] Wang Z, Ren Z, Chen Y, Hu J, Yang G, Yu L, Yang X, Huang A, Zhang X, Zhou S, Sun H, Wang Y, Ge N, Xu X, Tang Z, Lau W, Fan J, Wang J and Zhou J. Adjuvant transarterial chemoembolization for hbv-related hepatocellular carcinoma after resection: a randomized controlled study. Clin Cancer Res 2018; 24: 2074-2081.
- [16] Zhou X, Zhang C, Yang S, Yang L, Luo W, Zhang W, Zhang X and Chao J. Macrophage-derived MMP12 promotes fibrosis through sustained damage to endothelial cells. J Hazard Mater 2024; 461: 132733.
- [17] Salarian M, Ghim M, Toczek J, Han J, Weiss D, Spronck B, Ramachandra AB, Jung JJ, Kukreja G, Zhang J, Lakheram D, Kim SK, Humphrey JD and Sadeghi MM. Homeostatic, non-canonical role of macrophage elastase in vascular integrity. Circ Res 2023; 132: 432-448.
- [18] Gao H, Zhou X, Li H, Liu F, Zhu H, Song X, Niu Z, Ni Q, Yang C and Lu J. Role of matrix metallopeptidase 12 in the development of hepatocel-

- Iular carcinoma. J Invest Surg 2019; 34: 366-372.
- [19] He MK, Le Y, Zhang YF, Ouyang HY, Jian PE, Yu ZS, Wang LJ and Shi M. Matrix metalloproteinase 12 expression is associated with tumor FOXP3+ regulatory T cell infiltration and poor prognosis in hepatocellular carcinoma. Oncol Lett 2018; 16: 475-482.
- [20] Ng KT, Qi X, Kong KL, Cheung BY, Lo CM, Poon RT, Fan ST and Man K. Overexpression of matrix metalloproteinase-12 (MMP-12) correlates with poor prognosis of hepatocellular carcinoma. Eur J Cancer 2011; 47: 2299-2305.
- [21] Cong T, Yang C, Cao Q, Ren J, Luo Y, Yuan P, Zheng B, Liu Y, Yang H, Kang W, Ou A and Li X. The role of GNMT and MMP12 expression in determining TACE efficacy: validation at transcription and protein levels. J Hepatocell Carcinoma 2024; 11: 95-111.
- [22] Xie D, Shi J, Zhou J, Fan J and Gao Q. Clinical practice guidelines and real-life practice in hepatocellular carcinoma: a Chinese perspective. Clin Mol Hepatol 2023; 29: 206-216.
- [23] Sugioka A, Kato Y and Tanahashi Y. Systematic extrahepatic Glissonean pedicle isolation for anatomical liver resection based on Laennec's capsule: proposal of a novel comprehensive surgical anatomy of the liver. J Hepatobiliary Pancreat Sci 2017; 24: 17-23.
- [24] Hidaka M, Eguchi S, Okuda K, Beppu T, Shirabe K, Kondo K, Takami Y, Ohta M, Shiraishi M, Ueno S, Nanashima A, Noritomi T, Kitahara K and Fujioka H. Impact of anatomical resection for hepatocellular carcinoma with microportal invasion (vp1). Ann Surg 2020; 271: 339-346.
- [25] Llovet JM and Lencioni R. mRECIST for HCC: performance and novel refinements. J Hepatol 2020; 72: 288-306.
- [26] Liang PI, Wang YH, Wu TF, Wu WR, Liao AC, Shen KH, Hsing CH, Shiue YL, Huang HY, Hsu HP, Chen LT, Lin CY, Tai C, Wu JY and Li CF. IGFBP-5 overexpression as a poor prognostic factor in patients with urothelial carcinomas of upper urinary tracts and urinary bladder. J Clin Pathol 2013; 66: 573-582.
- [27] Yin JZ, Shi XQ, Wang MD, Du H, Zhao XW, Li B and Yang MH. Arsenic trioxide elicits anti-tumor activity by inhibiting polarization of M2like tumor-associated macrophages via Notch signaling pathway in lung adenocarcinoma. Int Immunopharmacol 2023; 117: 109899.
- [28] Cheng M, Xu J, Ding K, Zhang J, Lu W, Liu J, Gao J, Alugupalli KR and Liu H. Attenuation of relapsing fever neuroborreliosis in mice by IL-17A blockade. Proc Natl Acad Sci U S A 2022; 119: e2205460119.
- [29] Awad MM, Oxnard GR, Jackman DM, Savukoski DO, Hall D, Shivdasani P, Heng JC, Dahlberg

- SE, Janne PA, Verma S, Christensen J, Hammerman PS and Sholl LM. MET exon 14 mutations in non-small-cell lung cancer are associated with advanced age and stage-dependent met genomic amplification and c-met overexpression. J Clin Oncol 2016; 34: 721-730.
- [30] Wang Y, He X, Zhou C, Bai Y, Li T, Liu J, Ju S, Wang C, Xiang G and Xiong B. Nanoscale CaO(2) materials for synergistic transarterial chemoembolization in a VX2 orthotopic rabbit liver cancer model. Acta Biomater 2022; 154: 536-548.
- [31] Wei X, Zhao L, Ren R, Ji F, Xue S, Zhang J, Liu Z, Ma Z, Wang XW, Wong L, Liu N, Shi J, Guo X, Roessler S, Zheng X and Ji J. MiR-125b loss activated HIF1alpha/pAKT loop, leading to transarterial chemoembolization resistance in hepatocellular carcinoma. Hepatology 2021; 73: 1381-1398.
- [32] Blukacz L, Nuciforo S, Fucile G, Trulsson F, Duthaler U, Wieland S and Heim MH. Inhibition of the transmembrane transporter ABCB1 overcomes resistance to doxorubicin in patient-derived organoid models of HCC. Hepatol Commun 2024; 8: e0437.
- [33] Lencioni R, Petruzzi P and Crocetti L. Chemoembolization of hepatocellular carcinoma. Semin Intervent Radiol 2013; 30: 3-11.
- [34] Jia B, Zhao X, Wu D, Dong Z, Chi Y, Zhao J, Wu M, An T, Wang Y, Zhuo M, Li J, Chen X, Tian G, Long J, Yang X, Chen H, Wang J, Zhai X, Li S, Li J, Ma M, He Y, Kong L, Brcic L, Fang J and Wang Z. Identification of serum biomarkers to predict pemetrexed/platinum chemotherapy efficacy for advanced lung adenocarcinoma patients by data-independent acquisition (DIA) mass spectrometry analysis with parallel reaction monitoring (PRM) verification. Transl Lung Cancer Res 2021; 10: 981-994.
- [35] Mirastschijski U, Haaksma CJ, Tomasek JJ and Agren MS. Matrix metalloproteinase inhibitor GM 6001 attenuates keratinocyte migration, contraction and myofibroblast formation in skin wounds. Exp Cell Res 2004; 299: 465-475.
- [36] Vogel A, Cervantes A, Chau I, Daniele B, Llovet JM, Meyer T, Nault JC, Neumann U, Ricke J, Sangro B, Schirmacher P, Verslype C, Zech CJ, Arnold D and Martinelli E; ESMO Guidelines Committee. Hepatocellular carcinoma: ESMO Clinical Practice Guidelines for diagnosis, treatment and follow-up. Ann Oncol 2018; 29 Suppl 4: iv238-iv255.
- [37] Qian J, Shen Y, Cui L, Wu Z, Tu S, Lin W, Tang H, Hu Z, Liu L, Shen W, He Y and He K. Survival effects of postoperative adjuvant TACE in early-HCC patients with microvascular invasion: a multicenter propensity score matching. J Cancer 2024; 15: 68-78.

- [38] Luo L, Shan R, Cui L, Wu Z, Qian J, Tu S, Zhang W, Xiong Y, Lin W, Tang H, Zhang Y, Zhu J, Huang Z, Li Z, Mao S, Li H, Hu Z, Peng P, He K, Li Y, Liu L, Shen W and He Y. Postoperative adjuvant transarterial chemoembolisation improves survival of hepatocellular carcinoma patients with microvascular invasion: a multicenter retrospective cohort. United European Gastroenterol J 2023; 11: 228-241.
- [39] Wang PX, Sun YF, Zhou KQ, Cheng JW, Hu B, Guo W, Yin Y, Huang JF, Zhou J, Fan J, Cheung TT, Qu XD and Yang XR. Circulating tumor cells are an indicator for the administration of adjuvant transarterial chemoembolization in hepatocellular carcinoma: a single-center, retrospective, propensity-matched study. Clin Transl Med 2020; 10: e137.
- [40] Hu H, Han XK, Long XR, Fan J, Yan ZP, Wang JH and Liu R. Prognostic nomogram for post-surgical treatment with adjuvant TACE in hepatitis B Virus-related hepatocellular carcinoma. Oncotarget 2016; 7: 58302-58314.
- [41] Wu Z, Cui L, Qian J, Luo L, Tu S, Cheng F, Yuan L, Zhang W, Lin W, Tang H, Li X, Li H, Zhang Y, Zhu J, Li Y, Xiong Y, Hu Z, Peng P, He Y, Liu L, He K and Shen W. Efficacy of adjuvant TACE on the prognosis of patients with HCC after hepatectomy: a multicenter propensity score matching from China. BMC Cancer 2023; 23: 325.
- [42] Liang Y, Wang Z, Peng Y, Dai Z, Lai C, Qiu Y, Yao Y, Shi Y, Shang J and Huang X. Development of ensemble learning models for prognosis of hepatocellular carcinoma patients underwent postoperative adjuvant transarterial chemoembolization. Front Oncol 2023; 13: 1169102.
- [43] Xu JX, Qin SL, Wei HW, Chen YY, Peng YC and Qi LN. Prognostic factors and an innovative nomogram model for patients with hepatocellular carcinoma treated with postoperative adjuvant transarterial chemoembolization. Ann Med 2023: 55: 2199219.
- [44] Hu S, Gan W, Qiao L, Ye C, Wu D, Liao B, Yang X and Jiang X. A new prognostic algorithm predicting hcc recurrence in patients with barcelona clinic liver cancer stage b who received PA-TACE. Front Oncol 2021; 11: 742630.
- [45] Yu Lin MO, Sampath D, Bosykh DA, Wang C, Wang X, Subramaniam T, Han W, Hong W and Chakraborty S. YAP/TAZ drive agrin-matrix metalloproteinase 12-mediated diabetic skin wound healing. J Invest Dermatol 2025; 145: 155-170, e2.

- [46] Chakraborty S, Sampath D, Yu Lin MO, Bilton M, Huang CK, Nai MH, Njah K, Goy PA, Wang CC, Guccione E, Lim CT and Hong W. Agrin-Matrix Metalloproteinase-12 axis confers a mechanically competent microenvironment in skin wound healing. Nat Commun 2021; 12: 6349.
- [47] Xing H, Zhang WG, Cescon M, Liang L, Li C, Wang MD, Wu H, Lau WY, Zhou YH, Gu WM, Wang H, Chen TH, Zeng YY, Schwartz M, Pawlik TM, Serenari M, Shen F, Wu MC and Yang T. Defining and predicting early recurrence after liver resection of hepatocellular carcinoma: a multi-institutional study. HPB (Oxford) 2020; 22: 677-689.
- [48] Lee HY, Rhim H, Lee MW, Kim YS, Choi D, Park MJ, Kim YK, Kim SH and Lim HK. Early diffuse recurrence of hepatocellular carcinoma after percutaneous radiofrequency ablation: analysis of risk factors. Eur Radiol 2013; 23: 190-197.
- [49] Shimoda M, Tago K, Shiraki T, Mori S, Kato M, Aoki T and Kubota K. Risk factors for early recurrence of single lesion hepatocellular carcinoma after curative resection. World J Surg 2016; 40: 2466-2471.
- [50] Li H, Liang J, Wang J, Han J, Li S, Huang K and Liu C. Mex3a promotes oncogenesis through the RAP1/MAPK signaling pathway in colorectal cancer and is inhibited by hsa-miR-6887-3p. Cancer Commun (Lond) 2021; 41: 472-491.
- [51] Wang Z, Zhao P, Tian K, Qiao Z, Dong H, Li J, Guan Z, Su H, Song Y and Ma X. TMEM9 promotes lung adenocarcinoma progression via activating the MEK/ERK/STAT3 pathway to induce VEGF expression. Cell Death Dis 2024; 15: 295.
- [52] Guan C, Xiao Y, Li K, Wang T, Liang Y and Liao G. MMP-12 regulates proliferation of mouse macrophages via the ERK/P38 MAPK pathways during inflammation. Exp Cell Res 2019; 378: 182-190.